The effect of raw materials and mechanical activation stages on properties of foamed concrete

Janis Baronins[1*, 2, 7], Andrei Shishkin[2], Vitalijs Lusis[3], Chiara Giosuè[4], Dmitri Goljandin[5], Iveta Novakova[1], Sofija Kekez[1], Aleksandrs Korjakins[6], Dmitrijs Gorelikovs[7], Pavels Gavrilovs[2, 8]

[1]*Department of Building, Energy and Material Technology,*
UiT The Arctic University of Norway, N-8505 Narvik, Norway
[2]*Institute of Materials and Surface Engineering, Faculty of Natural Sciences and Technology,*
Riga Technical University, P. Valdena Str. 7, Riga, LV-1048, Latvia
[3]*Liepaja Study and Science Centre,*
Riga Technical University, Liedaga Street 3, Liepaja, LV-3416 Latvia
[4]*Department of Science and Engineering of Matter, Environment and Urban Planning (SIMAU),*
Università Politecnica delle Marche, INSTM research unit, Ancona, 60131, Italy
[5]*Department of Mechanical and Industrial Engineering,*
Tallinn University of Technology (TalTech), Ehitajate tee 5, Tallinn, 19086, Estonia
[6]*Institute of Materials and Structures,*
Riga Technical University, Kipsalas Street 6A, Riga, LV-1048, Latvia
[7]*Latvian Maritime Academy,*
Riga Technical University, Flotes Street 12 k – 1, Riga, LV-1016
[8]*Transport institute, Faculty of Civil and Mechanical Engineering,*
Riga Technical University, Kipsalas street 6a, Riga, LV-1048, Latvia

ABSTRACT

This study investigates the impact of high-energy milling on foamed concrete, which is crucial for its lightweight and insulating properties. The research uses a two-rotor disintegrator for milling cement, sand, and microsilica to evaluate the mechanical properties of foamed concrete produced with a high-speed homogenizer in a novel two-stage process. Comparisons are made between non-milled, single-milled, and double-milled individual components and mixtures with commercial binders. While energy consumption significantly increases after double-milling, immediate use of single-milled mixtures leads to enhanced compressive strength – 6.53 MPa for Portland-limestone cement and 9.95 MPa for white Portland cement. However, storing these mixtures for three days reduces their strength to 5.20 MPa and 6.63 MPa, respectively, due to reagglomeration. Microstructural analysis reveals finer particles and larger pores in samples made with milled mixtures, highlighting the importance of immediate use for optimal foamed concrete quality.

Keywords: foamed concrete; milling; binding energy; direct foaming; cavitation.

*Corresponding author: Janis Baronins (Janis.Baronins@uit.no).

1. INTRODUCTION

Choosing the suitable binder and methods enables the production of various porous concretes, such as foamed and autoclaved aerated concrete, crucial in civil and mechanical engineering, as shown in Figure 1 [1–3]. These materials, also known as foam concrete or lightweight cellular concrete, have densities between 0.4 to 1.6 g·cm^{-3}

and offer advantages such as low density, simple production, installation, and superior mechanical performance [4,5]. The air voids in hardened concrete have two distinct effects on its performance. On one hand, an increase in air content reduces strength and thermal conductivity [6]. On the other hand, their closed-cell structure ensures low water absorption, high resistance to freezing-thawing [7], superior thermal insulation, and reduced wetting-caused erosion-corrosion rate [8]. Rapidly producible and installable, foamed concrete blocks, with porosities of 10 to 60%, serve as effective insulators and barriers, featuring low density, high stiffness, and durability [9–12]. While mixing alkaline cement with aluminium powder enhances porosity, it increases costs and environmental risks due to excessive aluminium use, especially in aerated concretes [12,13]. Establishing an optimal air void system in foamed concrete is crucial to producing a material with a high strength-to-weight ratio [14].

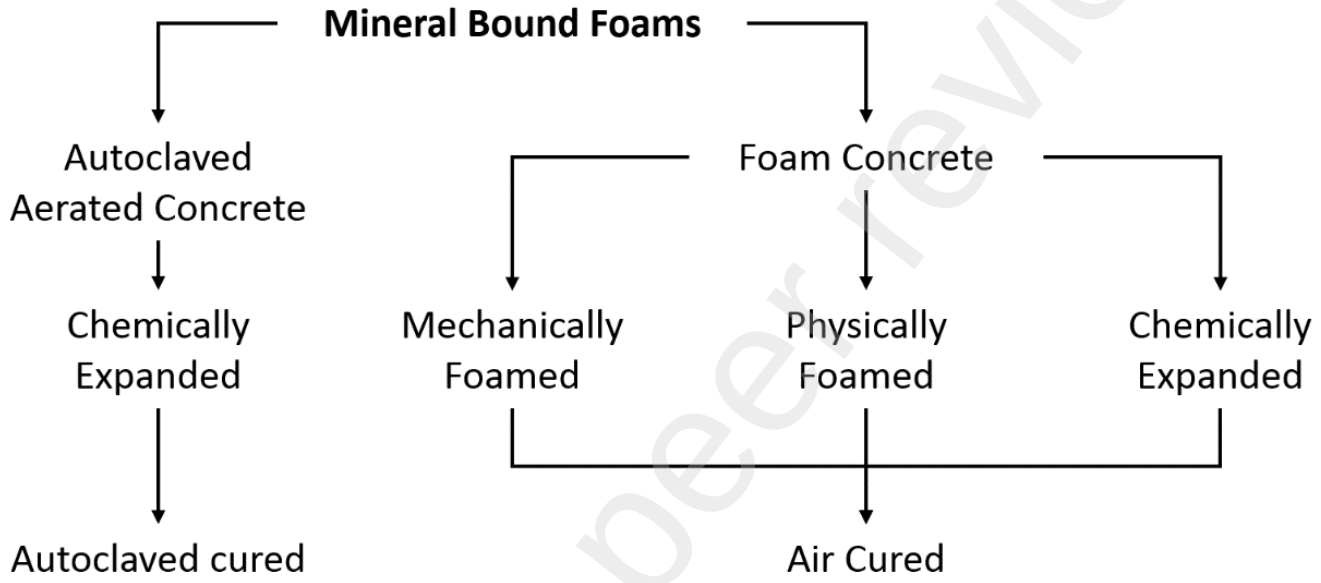

Figure 1. Comprehensive classification of mineral-bound foams: an extended scheme [15] based on selected manufacturing methods and literature review [16–18].

In tandem with initiatives aimed at generating alternative approaches to produce low-carbon cementitious materials and diminish the utilisation of sand and gravel resources [16], there is a critical need to innovate new energy-efficient technologies for aggregate preparation and foamed concrete production. Incorporating micro- or nanoscale fillers into polymer and concrete matrices is widely adopted for significantly enhancing their mechanical, electrical, and thermal properties, durability, strength, and environmental resistance to meet specific performance criteria [19]. These endeavours aim to propel the low-carbon transition and foster the sustainable development of foamed concrete [16].

Since 1925, two chemical reaction-free methods for manufacturing foamed concrete have been prominent: 1) mixing the pre-prepared foam with cement mortar, known as "physically foamed", and 2) adding a foaming agent directly to the cement mortar during intensive mechanical mixing referred to as "mechanically foamed". These are known as classical or two-stage ("pre-foaming") [17] and aeration ("mixed-foaming") [18] methods, respectively.

The "pre-foaming" method, patented for producing stable foam and fresh cement-sand mortar without high porosity, is complex and requires numerous steps and equipment, leading to extended production time and lower productivity. Furthermore, large grain sizes of cement and additives can disrupt the foam structure, posing additional challenges [20,21].

In the aeration method, simultaneous mixing, homogenisation, pore formation, and increased binding energy of milled particles occur in a high-speed mixer. This method has evolved with different mixer designs, employing turbulence to create homogeneously distributed air-filled pores [18,22]. The barotechnological process, involving mixing under high atmospheric pressure in a sealed chamber, further enhances this method by forming pores and swelling the mixture during slow pressure release [15,23].

Efficiency in foamed concrete production can be improved by combining aeration with the barotechnological process. Such an approach involves mixing main components with a foaming agent under high pressure, facilitating both vertical and horizontal transport of the foamed concrete. High-speed milling creates turbulence and cavitation, creating a more homogeneous product with increased reactivity and compressive strength [24,25].

The traditional method of using sand with cement for foam generation has evolved to include pozzolanic additives like microsilica, which fill spaces between larger cement grains, increasing the concrete matrix's packing density [18,26]. Achieving high homogenisation of microsilica in aqueous suspension is essential for a homogenous fresh cement mortar and requires a high-speed mixer-disperser (HSMD) [24,27,28]. The pozzolanic reaction between amorphous silica and calcium hydroxide enhances the cementitious effect, filling voids between cement grains and larger fillers [29].

Mechanical mixing of concrete and mortar for foaming necessitates suitable flowability. Polycarboxylate-based superplasticisers manage the tendency of cement particles to flocculate in water by increasing zeta potential and dispersing particles effectively [30–35].

A patented 3-stage production technology involves high-energy milling, homogenisation, and mixing-foaming [25,36]. It offers a refined porous structure but does not prevent the formation of larger pores. In-situ hydrophobisation methods for direct foaming of clay, Portland cement, and aluminate cement mortars modify wetting behaviour, stabilising pores but increasing the risk of excessively more extensive void formation [37–41]. Choosing and controlling foaming agent concentration is crucial for calcium aluminate-based mortars to maintain the desired porous structure without increasing water permeability [10,37,38,42].

The present research conducted experiments using a two-stage simulated process [43] with different types of cement to improve the foamed concrete's reactive and hardening characteristics. The selected approach involved crushing and activating dry components, then mixing them with water and a foaming agent at high speeds to optimise the pozzolanic reaction during hardening [44]. Since dry raw materials are frequently milled and utilised at separate intervals, primarily due to storage and transportation logistics, it became imperative to examine the influence of short-term storage of these milled materials on the workability and characteristics of cement mortars and foamed concrete.

2. EXPERIMENTAL

2.1 Applied materials

Three commercially available types of cement served as binders: Portland-limestone cement (PLC) CEM II/A-LL 42,5N (SCHWENK Latvija, Broceni, Latvia), white Portland cement (WPC) Aalborg White CEM I 52,5R (Aalborg Portland Polska Sp.zo.o., Warszawa, Poland), and calcium aluminate cement (CAC) GÓRKAL 70 (Górka Cement, Trzebinia, Poland). Their compositions, determined via X-ray fluorescence (XRF) Rigaku Supermini (Rigaku Corporation, Tokyo, Japan), are detailed in Table 1. As the matrix aggregate, sieved quartz sand (Sakret Ltd, Riga, Latvia) with particle sizes up to 0.1 mm was used (Sand Raw). To ensure high pozzolanic activity, Microsilica (silica fume) Grade 92D (Cilantro Chemicals Pvt. Ltd., Navi Mumbai, India) was added. The polycarboxylate-based Sikament® 56 superplasticiser (SIKA Baltic SIA, Riga, Latvia) [45] reduced the water-to-cement ratio for fresh cement mortar preparation. The synergistic blend of anionic surfactants and functional additives, including the foaming agent FAB-12A (E Lade SIA, Riga, Latvia) [46], performed the stabilisation and enhancement of properties.

Table 1 The study determined the comparative properties of PLC, WPC [13], and CAC [47] using XRF and collecting data from literature sources.

Component	PLC	WPC	CAC
CaO, wt.%	48.83	68.9	28-30
Al_2O_3, wt.%	7.77	Not specified	69-71
SiO_2, wt.%	31.09	24.8	<0.5
Al_2O_3 + Fe_2O_3, wt.%	9.92	2.20	<0.3
MgO, wt.%	6.26	0.52	Not specified
SO_3, wt.%	3.5	2.20	Not specified
K_2O+Na_2O, wt.%	>0.85	0.27	<0.5
LOI	Not specified	0.14	Not specified
Specific gravity (kg·cm^{-3})	3200	3150	3000
Setting time, initial (min)	60	120	>160

2.2 Applied method for two-stage preparation of dry materials

A two-stage approach [43] was employed to produce foamed concrete specimens, as outlined in Figure 2.

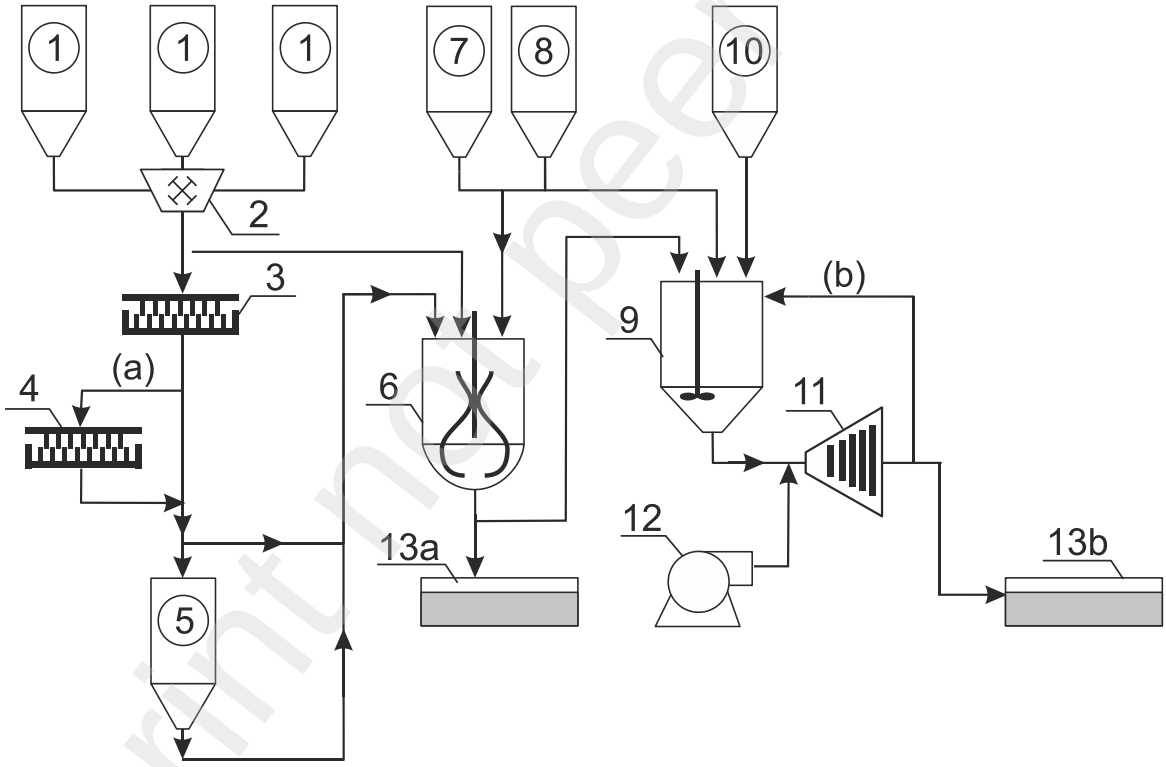

Figure 2. Schematic of the two-stage foamed concrete production process. Key components include: 1 – containers for dry components (cement, sand, microsilica); 2 – V-type mixer for initial mixing of raw minerals; 3 and 4 – disintegrator; 5 – container for storing powdered mix; 6 – mortar mixer for creating flowable cement mortar paste; 7, 8, and 10 – containers for water, superplasticiser, and foaming agent respectively; 9 – mixer-reactor; 11 – high-speed mixer-disperser (HSMD); 12 – air compressor; 13a and 13b – moulds for solid mortars and foamed concrete. Channels (a) and (b) represent the flow/recirculation paths for milling and foaming stages.

Initially, 30 kg of dry components were collected from containers, as illustrated in Figure 2 – 1, weighed according to the mixture design in Table 2, and then mixed for 3 minutes at 42 min^{-1} in a V Type Powder Mixer Machine (Wuxi Nuoya Machinery Co., Ltd, Jiangsu, China), as depicted in Figure 2 – 2. A semi-industrial-scale DSL-115

two-rotor disintegrator (Tallinn University of Technology, Estonia, Figure 2 – 3) [48] processed these components at a maximum speed of 12,000 min^{-1}, achieving an impact velocity of up to 192 $m \cdot s^{-1}$. The process immediately transfers single-milled (X1) materials to the mixer (Figure 2 – 6) or stores them for three days in a closed container (Figure 2 – 5). The procedure rerouted double-milled (X2) mixtures through another disintegrator, DSL-115 (Figure 2 – 4), before mixing (Figure 2 – 6) or storage (Figure 2 – 5). The study also subjected Sand Raw to a triple-milling process (X3) to assess the impact of energy input on sand particle fineness and its potential to reduce foamed concrete manufacturing costs. However, Sand X3 was not used in foamed concrete production. The analysis compared X1, X2 and X3 mixtures and individual components against their non-milled (NM) counterparts.

The Clatronic Multi Food Processor KM3350 anchor-type mixer (Clatronic International GmbH, Germany, Figure 2 – 6) first moistened the X1 mixtures at 40 min^{-1}. Half the total water weight and all the calculated superplasticizer from containers (Figure 2 – 7 and 8) were added and mixed for 5 minutes, forming a flowable cement mortar paste. This mortar paste was gradually transferred to the mixer-reactor (Figure 2 – 9) over 90 seconds, with the remaining water added (Figure 2 – 7). The KMD 1,5 HSMD (Riga Technical University, Latvia, Figure 2 – 11) then mixed the mortar at increasing rotation speed up to 5000 min^{-1}, reaching linear speed of cavitation blades up to 80 $m \cdot s^{-1}$ for 90 seconds. During recirculation through channel (b), the liquid pump added the foaming agent from the container (Figure 2 – 10). After five recirculation cycles, air from the compressor (Figure 2 – 12) doubled the mortar volume in the reactor (Figure 2 – 9). This foamed mortar underwent five more cycles before being poured into 30x30x300 mm (±1 mm) prism-shaped plywood moulds (Figure 2 – 13b), vibrated for 10 seconds, and then covered and stored at room temperature in sealed plastic boxes for 3, 7, 28, and 56 days to maintain moisture. These foamed specimens were labelled "Foam", as shown in Table 3.

Table 2 Mixture designs applied for milling, cement mortar production, and foamed concrete manufacturing processes.

Component	Concentration, wt.% (dry components)	Concentration, wt.% (cement mortar)	Concentration, wt.% (foamed concrete)
Cement	41	32.9	32.9
Sand	52	44.2	42.6
Microsilica	7	5.8	5.8
Water	-	16.3	16.3
Superplasticizer	-	0.8	0.8
Foaming agent	-	0	1.6
Water to cement ratio	-	0.5	0.5

Table 3 Designations of hardened specimens based on milling cycles (NM, X1 and X2), storage duration of milled powder (0 and 3 days), and foaming status (Foam).

	Cement mortar					Foamed concrete	
Storage duration (dry*)	0 days**			3 days		0 days	3 days
Nº of milling cycles	0	1	2	1	2	1	1
Cement type and brand							
PLC CEM II/A-LL 42,5N	PLC-NM	PLC0-X1	PLC0-X2	PLC3-X1	PLC3-X2	PLC0-X1 Foam	PLC3-X1 Foam
WPC CEM I 52,5R	WPC-NM	WPC0-X1	WPC0-X2	WPC3-X1	WPC3-X2	WPC0-X1 Foam	WPC3-X1 Foam
CAC GÓRKAL 70	CAC-NM	CAC0-X1	CAC0-X2	CAC3-X1	CAC3-X2	~~CAC0-X1 Foam~~***	~~CAC3-X1 Foam~~***

* Storage of dry components after milling before use.
** Immediately used for cement mortar and foamed concrete production.
*** The output of foamed samples failed with the selected method and materials.

The system maintained the curing and storage conditions at a temperature of 20 °C (±2 °C) and a relative humidity of 95% (±3%). All specimens were allowed to harden for three days before being demoulded. The protocol required submerging selected specimens in water. It scheduled tests for 3- (cement mortars only), 7-, 28-, and 56-day intervals after casting to ensure complete cement hydration throughout the curing period.

2.3 Applied method for granulometric analysis of milled powders

The particle size distribution of the dry components was analysed in three different states: NM, after X1, and following X2, using a disintegrator, as illustrated in Figure 2 – sections 2, 3, and 4, respectively. The Analysette 3 sieve shaker (FRITSCH GmbH, Idar-Oberstein, Germany) performed the fractioning, utilising sieves with mesh openings of various sizes (0.054, 0.0765, 0.1075, 0.1875, 0.375, 0.605, and 0.855 mm). Additionally, to extend the measurement capabilities to as small as 0.1 μm, the results were augmented with data from the Analysette 22 NanoTec laser particle sizer (FRITSCH GmbH, Idar-Oberstein, Germany)

The particle size distributions of Sand Raw, along with sand subjected to X1 (Sand X1), X2 (Sand X2) and X3 (Sand X3), were analysed to assess the impact of milling cycles. This analysis aimed to provide a comprehensive understanding of the influence of milling on particle size distribution and establish a correlation between Sand X1 and Sand X2 with the mechanical and morphological properties of the resultant foamed concrete. The degree of milling (n) was determined using Equation (1) from reference [49]:

$$n = D_{50} \cdot d_{50}^{-1} \quad (1)$$

where: D_{50} – measured median particle size before milling, mm.

d_{50} – measured median particle size after milling, mm.

2.4 Applied methods for compressive strength, density, and morphology analysis of cement mortar

A wet-cut tabletop concrete saw cut prism-shaped specimens of solid mortar into cubes measuring 30x30 mm (±1.5 mm). After hardening for 3, 7, 28, and 56 days, the process involved removing these samples from a temperature-controlled water container and subjecting them to testing. Cement mortar specimens underwent compressive strength tests three days after casting, with NM mixtures-based specimens additionally tested after 14 days. The compressive strength of these specimens was measured using an Instron 8801 Universal Testing Machine (Instron, Norwood, USA) at a controlled room temperature of 20 °C (±2 °C). The testing proceeded at a consistent quasi-static speed of 3 $mm \cdot min^{-1}$, with the reported results representing the average values derived from seven replicates for each mixture. The reported results represent the average values derived from seven replicates for each mixture. The process applied Archimedes' principle to assess the apparent density and porosity of the hardened mortars, documenting the average results from seven samples of each mixture. A Keyence VHX-2000 digital optical microscope (Keyence Corp, Osaka, Japan), equipped with a high-resolution 54 Mpix camera and a VH-Z20R/Z20W lens (Keyence Corp, Osaka, Japan), facilitated rigorous examinations of the surface morphologies of both unprocessed and fractured samples.

2.5 Applied method for water uptake and Archimedes tests

The water uptake capacity of the fabricated materials was ascertained via modified and reversed water uptake test [27] at a controlled temperature of 20 °C (±5 °C). Specimens underwent retrieval from the water after a 56-day immersion period. Their weight in air and submerged in water was measured using a Kern EW600-2M scale (KERN & SOHN GmbH, Balingen, Germany, ±0.01g accuracy). Following this, the samples were placed in a climate chamber for 72 hours at 20 °C (±1 °C) and 75% (±5%) relative humidity to facilitate mild drying conditions. Subsequently, the specimens underwent transfer to a Memmert ULE 400 oven (Memmert GmbH, Schwabach, Germany), where the heater incrementally raised the temperature to 65 °C (±2 °C) for the initial 24 hours and subsequently to 85 °C (±2 °C) for the next 24 hours. This approach aims to protect samples from high-temperature gradient formation and minimize the risk of generating new defects due to water vapour and gas

accumulation in the cement mortar and foamed concrete samples. Higher temperature (~90 °C) regimes would lead to bond water loss [50]. After the drying process, the specimens cooled to room temperature in desiccators. The recording of the final weight of the dried samples occurred in the air. A sample achieves dryness when the variance in its monitored weight within the desiccator over 24 hours is less than 0.1%.

The procedure underwent replication seven times to ensure the reliability of the reported average results. Subsequently, the designated equation (2) was employed to calculate the absolute weight of water absorbed by the specimens.

$$\frac{\Delta M}{M_0}(\%) = \frac{M_w - M_0}{M_0} \cdot 100 \quad (2)$$

where: M_w – weight of sample after immersion.

M_0 – weight of dried sample.

ΔM – the difference in the weight of sample during drying.

3. RESULTS

3.1 Effect of milling stages on energy use and median particle sizes in dry components and mixtures

The evaluation of median particle sizes and process efficiencies for different raw components, after preliminary mixing and the X1 and X2 processes, is presented in Table 4. Tested sand was additionally X3. Materials analysed included sand, microsilica, PLC, WPC, and CAC, focusing on the changes in particle size, degree of milling, and the energy requirements associated with these processes.

The results indicate a substantial reduction in measured median particle size for all components after milling, with tested sand exhibiting the most significant decrease from 0.435 mm ($D_{50\_Sand\ Raw}$) to 0.096 mm ($d_{50\_Sand\ X2}$) after X2 and to 0.067 mm ($d_{50\_Sand\ X3}$) after X3. This trend of consistent particle size diminution across various materials confirms the efficacy of the milling process in reducing particle size. However, the degree of milling varied across materials. Sand showed the highest degree at 4.54 after X2 and 6.52 after X3, suggesting a higher susceptibility to particle size reduction through milling than other materials. In contrast, materials such as PLC and WPC, although achieving finer particles after milling, showed relatively lower degrees of milling from 1.09 (PLC X1) to 1.97 (WPC X2).

The study also observed an incremental increase in energy requirements with successive milling processes. Specifically, the energy required for milling sand doubled from 4.3 $kW \cdot h \cdot T^{-1}$ (X1) to 8.6 $kW \cdot h \cdot T^{-1}$ (X2). This trend was consistent across all components, indicating a direct correlation between achieving finer particles and increased energy consumption under selected feeding rates of materials.

Table 4. Comparative analysis of median particle sizes and process efficiencies for milling components. This table presents the median particle sizes of individual components that were subjected to X1 and X2 (sand was additionally subjected to X3). Further, it details the degree of milling and quantifies the energy required for the milling process.

Dry components or mixture	Measured median particle size before milling, D_{50}	Measured median particle size after milling, d_{50}	Degree of milling, n	Required energy for milling	
	mm	mm		$kW \cdot h \cdot T^{-1}$	$kJ \cdot kg^{-1}$
Sand Raw	0.435	-	-	-	-
Sand X1	-	0.149	2.92	4.3	15.48
Sand X2	-	0.096	4.54	8.6	30.96
Sand X3	-	0.067	6.52	12.9	46.44
Microsilica Raw	0.11	-	-	-	-
Microsilica X1	-	0.049	2.29	4.3	15.48
Microsilica X2	-	0.040	2.73	8.6	30.96
PLC Raw	0.020	-	-	-	-
PLC X1	-	0.018	1.09	4.3	15.48
PLC X2	-	0.016	1.22	8.6	30.96
WPC Raw	0.016	-	-	-	-
WPC X1	-	0.011	1.41	4.3	15.48
WPC X2	-	0.008	1.97	8.6	30.96
CAC Raw	0.016	-	-	-	-
CAC X1	-	0.013	1.21	4.3	15.48
CAC X2	-	0.011	1.38	8.6	30.96

The median particle sizes and process efficiencies for cements containing component mixtures were evaluated after preliminary mixing (PLC Mix Raw, WPC Mix Raw, and CAC Mix Raw) and subsequent X1 (PLC Mix X1, WPC Mix X1, and CAC Mix X1) and X2 (PLC Mix X2, WPC Mix X2, and CAC Mix X2), as shown in Table 5. The focus was on changes in particle size, the degree of milling, and energy requirements associated with the processes.

The results demonstrate a consistent reduction in particle size across all tested mixtures after milling. PLC Mix's median particle size decreased from 0.094 mm ($D_{50\_PLC\ Mix\ Raw}$) to 0.044 mm ($d_{50\_PLC\ Mix\ X2}$) after X2. Similarly, WPC and CAC based mixtures also showed notable reductions in particle sizes, confirming the milling process's effectiveness in particle size diminution. The degree of milling varied across materials, with WPC based mixtures showing the highest degree at 2.24 after X2 (WPC Mix X2), suggesting different susceptibilities to particle size reduction through milling.

For mixing without milling, PLC Mix Raw, WPC Mix Raw, and CAC Mix Raw require 2.15 $kW \cdot h \cdot T^{-1}$, indicating an initial energy investment even before milling. As expected, the energy required for milling increased with successive milling. For instance, the energy for milling PLC based mixtures doubled from 4.3 $kW \cdot h \cdot T^{-1}$ (PLC Mix X1) to 8.6 $kW \cdot h \cdot T^{-1}$ (PLC Mix X2), a trend consistent across all mixtures. This highlights a direct correlation between achieving finer particles and increased energy and material consumption at the selected working conditions.

This comparative analysis of median particle sizes and process efficiencies for raw components and component mixtures offers valuable insights into the milling process's impact on particle size reduction and the associated energy costs. The consistent decrease in particle size after milling across various materials confirms the process's efficacy. Yet the varied degree of milling suggests that different materials respond differently due to their inherent

properties. Furthermore, this inconsistency indicates that factors at the crystalline or structural level might significantly influence the milling efficiency [51].

Table 5. Comparative analysis of cements-containing components mixtures median particle sizes and mixing-milling process efficiencies. This table presents the median particle sizes of preliminarily mixed component mixtures (Mix Raw) followed by those subjected to X1 and X2. Additionally, it details the degree of milling and quantifies the energy required for mixing and milling processes.

Dry cements containing mixtures	Measured median particle size before milling, D_{50}	Measured median particle size after milling, d_{50}	Degree of milling, n	Required energy for mixing without milling		Required energy for milling	
	mm	mm		$kW \cdot h \cdot T^{-1}$	$kJ \cdot kg^{-1}$	$kW \cdot h \cdot T^{-1}$	$kJ \cdot kg^{-1}$
PLC Mix Raw	0.094	-	-	2.15	7.74	-	-
PLC Mix X1	-	0.066	1.42	-	-	4.3	15.48
PLC Mix X2	-	0.044	2.14	-	-	8.6	30.96
WPC Mix Raw	0.092	-	-	2.15	7.74	-	-
WPC Mix X1	-	0.057	1.61	-	-	4.3	15.48
WPC Mix X2	-	0.041	2.24	-	-	8.6	30.96
CAC Mix Raw	0.092	-	-	2.15	7.74	-	-
CAC Mix X1	-	0.058	1.59	-	-	4.3	15.48
CAC Mix X2	-	0.042	2.19	-	-	8.6	30.96

The increased energy requirement for achieving finer particles is a significant consideration, presenting a trade-off between desired fineness and higher energy consumption. This trade-off necessitates a balanced approach, particularly in the context of environmental sustainability and operational costs. While smaller particles are often desirable for industrial applications, the environmental implications and energy costs cannot be overlooked [52].

3.2 Effect of milling stages on particle size distribution in dry components and mixtures

The Sand Raw exhibits a peak concentration of measured particle sizes (54.8 wt.%) at 0.375 mm. This peak diminishes significantly to 12.5, 3.9, and 0.8 wt.% in Sand X1, Sand X2, and Sand X3, respectively, as depicted in Figure 3. The milling process forms three distinct peaks in the finer particle size concentration range at 0.035, 0.0765, and 0.1875 mm. While X1 and X2 result in maximum detectable particle sizes of up to 0.605 mm, X3 reduces the maximum particle size to 0.375 mm as determined by the employed sieve analysis technique. X2 leads to a more uniform particle size distribution, potentially offering a more efficient reinforcement effect in foamed cement mortar and cemented sand structures [53] at optimal energy consumption for milling compared to X3 sand. Consequently, the study focuses on estimating the impact of X1 and X2 efficiency and the properties of hardened foamed mortars. This approach balances particle size refinement with energy efficiency and structural performance.

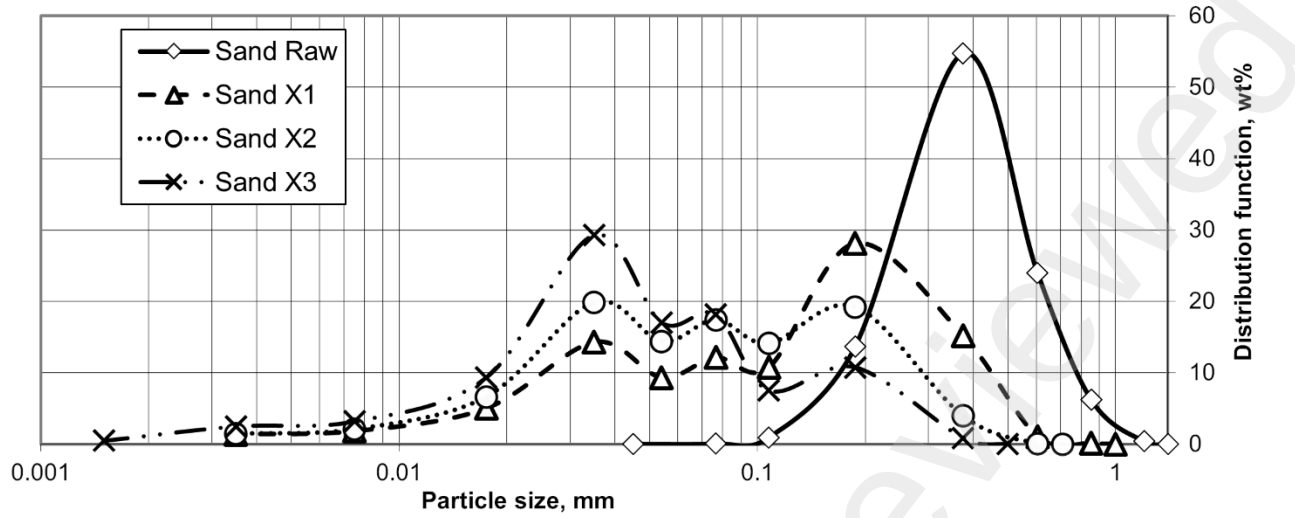

Figure 3. Particle size distribution of Sand Raw and after X1, X2, and X3 processes.

The tested microsilica's median particle size was determined to be $D_{50\_Microsilica\ Raw} = 0.11$ mm. Subsequent X1 and X2 processes resulted in an increased, yet similar, degree of milling, with $n_{Microsilica\ X1} \approx 2.23$ and $n_{Microsilica\ X2} \approx 2.73$. Notably, X1 markedly reduced the concentration of larger particles ranging from 0.0765 to 0.375 mm compared to the Microsilica Raw. However, X2 did not significantly alter the particle size distribution, as depicted in Figure 4. This milling process also increased the proportion of finer particles ($d_{50\_Microsilica\ X1} \approx 0.049$ mm and $d_{50\_Microsilica\ X2} \approx 0.040$ mm) relative to the Microsilica Raw.

The Microsilica Raw exhibited concentration peaks of 10.7, 21.6, and 27 wt.% at particle sizes of 0.035, 0.0765, and 0.185 mm, respectively. After milling, the latter two peaks diminished to approximately 5.3 and 3.7 wt.%, leading to a notable increase in concentration up to 25.2 wt.% (at 0.0175 mm) in the particle size range from 0.0015 to 0.054 mm, as illustrated in Figure 4.

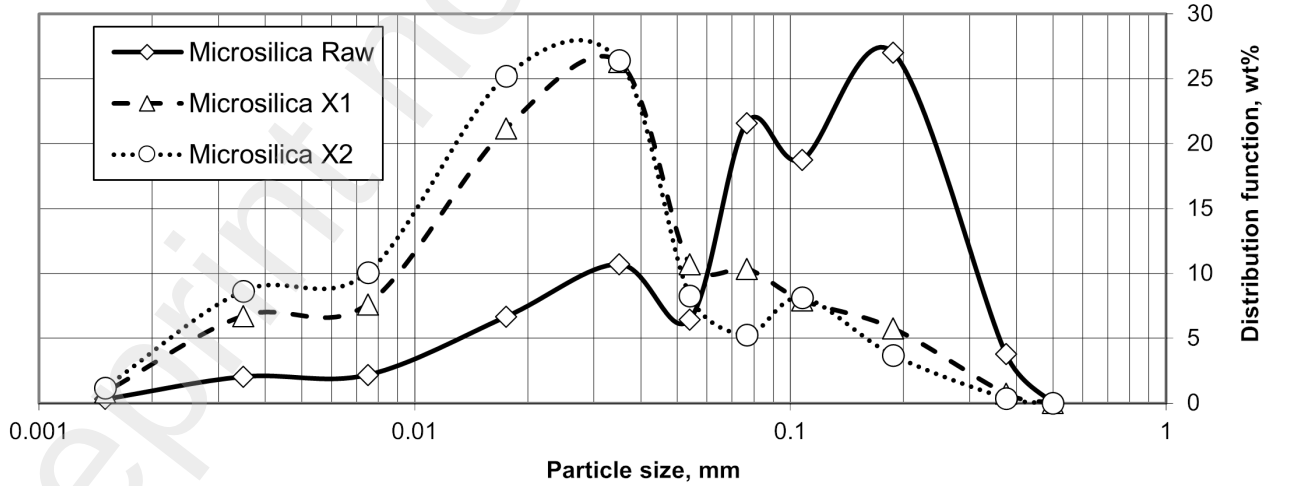

Figure 4. Particle size distribution of Microsilica Raw, Microsilica X1 and Microsilica X2.

It's recognized that milled microsilica contains a higher content of the amorphous phase than Microsilica Raw and leads to a 34-46% increase in the compressive strength of hardened cement mortars due to intensified alkali-silica reactions during the early hardening stage. However, it's been observed that this approach typically doesn't

significantly impact the compressive strength of hardened mortars compared to microsilica produced by the classification (sieving) method and subsequent storage under the same environmental conditions [54]. Additionally, storing in environments with high humidity levels (above 30%) diminishes the pozzolanic properties of microsilica in a relatively short time due to the formation of agglomerates. This effect also complicates the dispersion of microsilica in cement mortar and foamed concrete matrix [55].

Consequently, milling results indicate a potentially significant effect from microsilica addition in foamed mortars made of raw and milled mixtures. However, no substantial effect is anticipated in the properties of foamed mortars composed of X1 and X2 cement-sand-microsilica mixtures due to the measured similarity in particle sizes and distribution [56]. Therefore, a notable effect of microsilica addition on the compressive strength of foamed mortars can be anticipated based on the milling results.

The granulometric analysis of the PLC Raw, WPC Raw, and CAC Raw reveals relatively similar particle size distribution and concentration patterns, as illustrated in Figure 5 a, b, and c, respectively. The predominant concentration peaks range from 0.0075 mm (WPC Raw at 24.6 wt.%) to 0.0175 mm (PLC Raw at 35.4 wt.% and CAC Raw at 31.2 wt.%). These findings also highlight very similar median particle sizes for the tested cements, spanning from 0.016 mm ($D_{50\_WPC\ Raw}$ and $D_{50\_CAC\ Raw}$) to 0.020 mm ($D_{50\_PLC\ Raw}$), as shown in Table 4. The largest particle sizes detected, ranging from 0.077 mm (WPC Raw) to 0.090 mm (PLC Raw and CAC Raw), represented minor concentrations (less than 0.2 wt.%) according to the chosen particle size analysis method, as demonstrated in Figure 5 b, a and c.

Upon X1 of the tested cements, there's generally an increase in the same peak concentrations, rising to 41.7 wt.% for WPC X1 and 39.7 wt.% for CAC X1. This trend suggests a decrease in concentrations of particles larger than 0.018 mm (Figure 5 a and c). Notably, the milling affects particles ranging from 0.018 to 0.035 mm, as evidenced by a decrease in concentrations within this range and a new peak at 0.004 mm for PLC X1 (Figure 5 b). The observed effect suggests the milling's destructive impact, particularly on WPC X1 and WPC X2 particles larger than 0.01 mm, under the applied energy for X1 (4.3 $kW \cdot h \cdot T^{-1}$) and X2 (8.6 $kW \cdot h \cdot T^{-1}$), respectively, as demonstrated in Table 4.

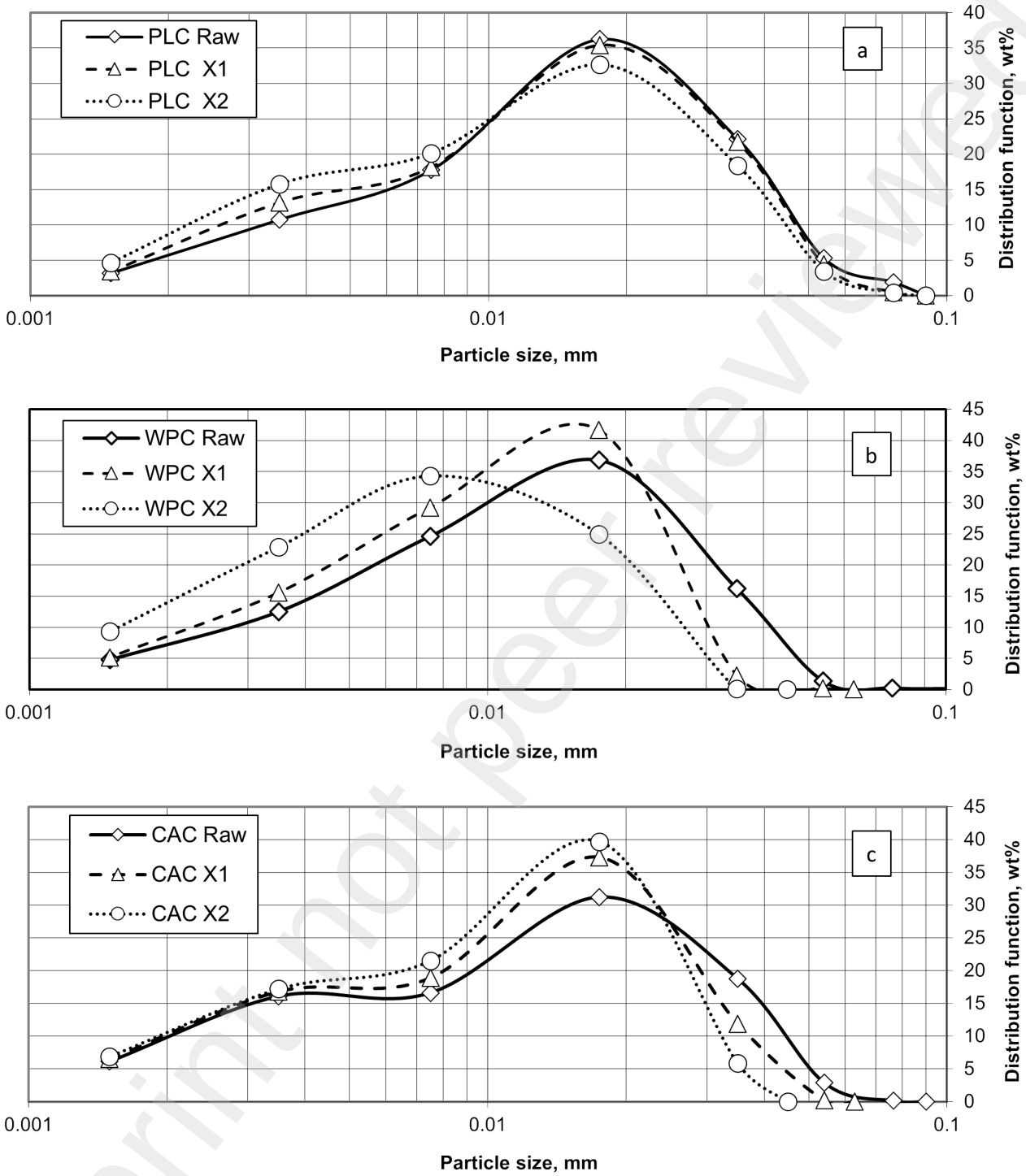

Figure 5. Particle size distribution for as-received (Raw), X1 and X2 milled PLC (a), WPC (b), and CAC (c) cements.

The particle size distributions for premixed (Mix Raw), X1, and X2 sand-microsilica-cement dry mixtures composed of PLC, WPC, and CAC are depicted in Figure 6 a, b, and c, respectively. After mechanical mixing and milling procedures, the granulometric distribution curves reveal the relationship between concentration peaks and the applied components.

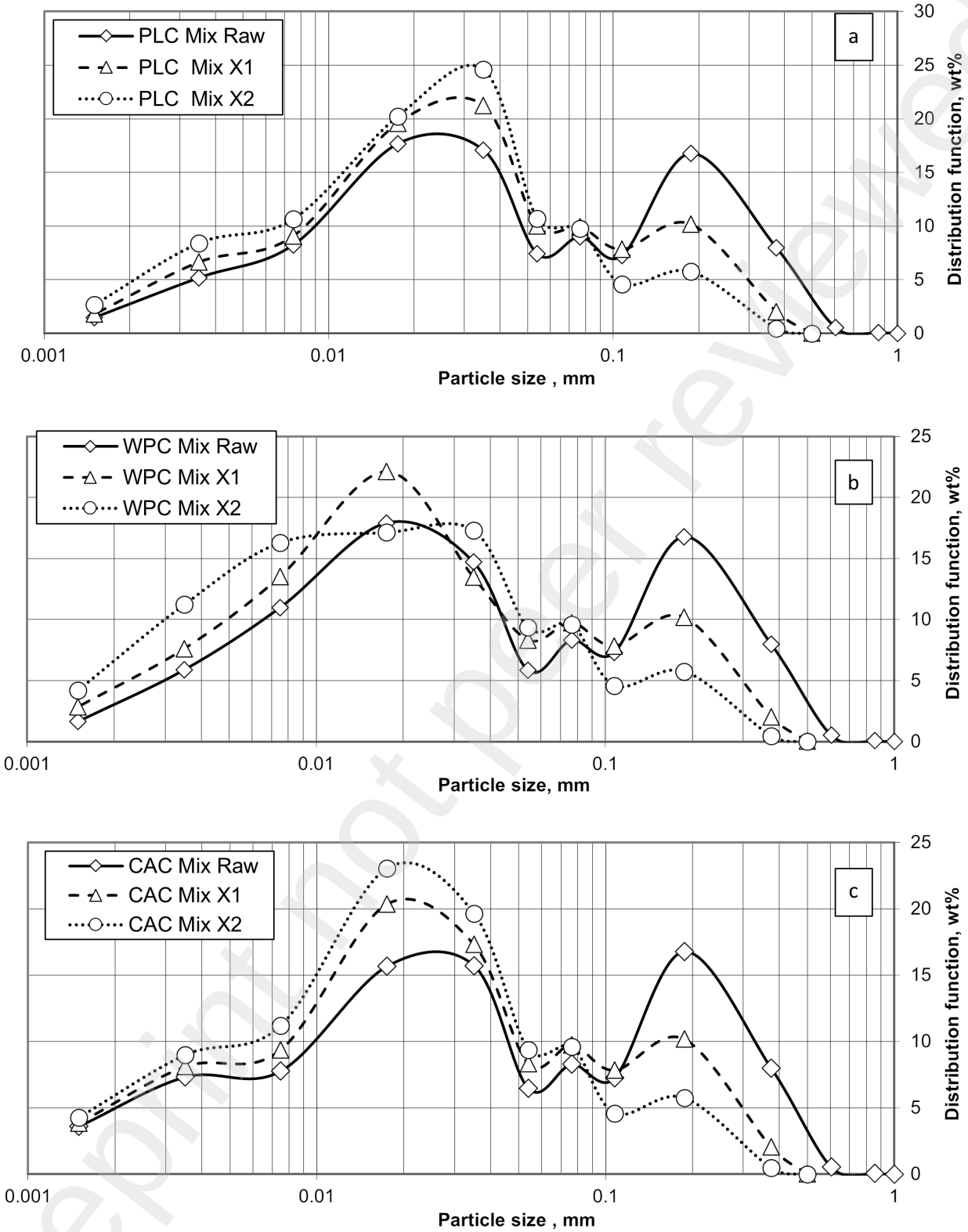

Figure 6. Particle size distribution of sand-microsilica-cement mixtures: premixed (Mix Raw) and after X1(Mix X1) and X2 (Mix X2) in compositions with PLC (a), WPC (b), and CAC (c).

Typical peaks in the granulometric analysis of raw and milled sand and microsilica were identified, with concentration maximums at 0.077 and 0.185 mm, respectively. Mixing and milling also alter concentration peaks

in the finer particle size range, primarily associated with raw and milled cement and micro silica. Considering that the microstructure of cement mortars typically demands reinforcing particles [57], X1 mixtures emerged as the preferred choice for producing foamed cement samples. The observation that X1 mixtures provide a more uniform particle size distribution across the entire tested range than X2 mixtures drove this choice. This uniformity is crucial for the cement mortars' desired reinforcement effect and overall performance. Additionally, cement particles with a diameter from 10 μm to 20 μm are crucial in determining the early compressive strength. In contrast, particles sized between 20 μm and 30 μm significantly impact the compressive strength at later stages [56].

The observed peak at 0.188 mm for sand remains noticeable for X1 and X2 dry component mixtures with micro silica and cement, as illustrated in Figure 6 a, b, and c. Mixtures WPC Mix X1 and CAC Mix X1 show a similar proportion of coarser sand particles, with a maximum concentration of 20% at a particle size of 0.188 mm. However, the WPC Mix X1 has a higher concentration (16.1%) of finer particles at 0.018 mm compared to the CAC Mix X1, which peaks (14%) at 0.035 mm. The prominence of coarser sand in PLC-containing samples diminishes to 9.7% due to a more significant presence of finer particles ranging from 0.018 to 0.108 mm, with a noticeable peak at 0.035 mm (17.9%). Additionally, the persistence of coarser sand particles at 0.375 mm (8.7%) and 0.605 mm (4.5%) might indicate a protective (cushioning) effect from PLC particles during X1 [58].

A similar phenomenon is observed after X2 of PLC and CAC containing mixtures, suggesting an impact probability effect on coarser sand particles by the milling elements. X2 of PLC containing mixtures results in an approximately 1.5-fold increase in the finest particle concentration (0.001 to 0.018 mm) compared to the result of X1. In contrast, X2 of CAC containing mixtures leads to a heightened concentration of the finest particles (0.018 to 0.077 mm) with a peak concentration (22.8%) at 0.035 mm, indicating a more pronounced effect on reducing of coarser sand particle sizes. The X2 of WPC containing mixtures increases (about 1.2 times) the concentration of finer particles in the size range from 0.001 to 0.054 mm.

In conclusion, the X2 stage does not significantly alter the particle size distribution of the selected sand. It may provide the most substantial coarse grain reinforcement effect in the tested hardened foamed concrete made of WPC and CAC containing mixtures after X1 compared to other specimens. This fact suggests that while X2 can increase the fineness of particles, X1 may be more effective for achieving a balance between fine and coarse particles for optimal reinforcement in foamed concrete.

Figure 7 demonstrates the effect of milling on the median particle size diameter (D50, d50). Sand, when subjected to milling, initially showed a decrease in particle size from 0.435 mm (0 millings, Sand Raw) to 0.149 mm (1 milling, Sand X1), followed by a reduction to 0.096 mm (2 millings, Sand X2) and further to 0.067 mm (3 millings, Sand X3). This trend suggests an initial agglomeration followed by effective size reduction upon further milling. For microsilica, a consistent decrease in particle size was observed with each milling, indicating a straightforward reduction from 0.110 mm (0 millings, Microsilica Raw) to 0.049 mm (1 milling, Microsilica X1) and then to 0.040 mm (2 millings, Microsilica X2). This behaviour points to microsilica's effective breakdown with milling.

PLC, WPC, and CAC also demonstrated a decrease in particle size with milling. PLC reduced from 0.02 mm (0 millings, PLC Raw) to 0.016 mm (2 millings, PLC X2), WPC from 0.016 mm (WPC Raw) to 0.008 mm (WPC X2), and CAC from 0.016 mm (CAC Raw) to 0.011 mm (CAC X2). The mixtures involving tested types of cement with sand and microsilica (PLC Mix, WPC Mix, and CAC Mix) showed similar trends, with significant reductions in particle size with each milling iteration. These results suggest that milling refines the particle size of both individual components and their mixtures, which could have implications for their application in cement mortar and foamed concrete construction materials, influencing properties such as reactivity, strength, and homogeneity.

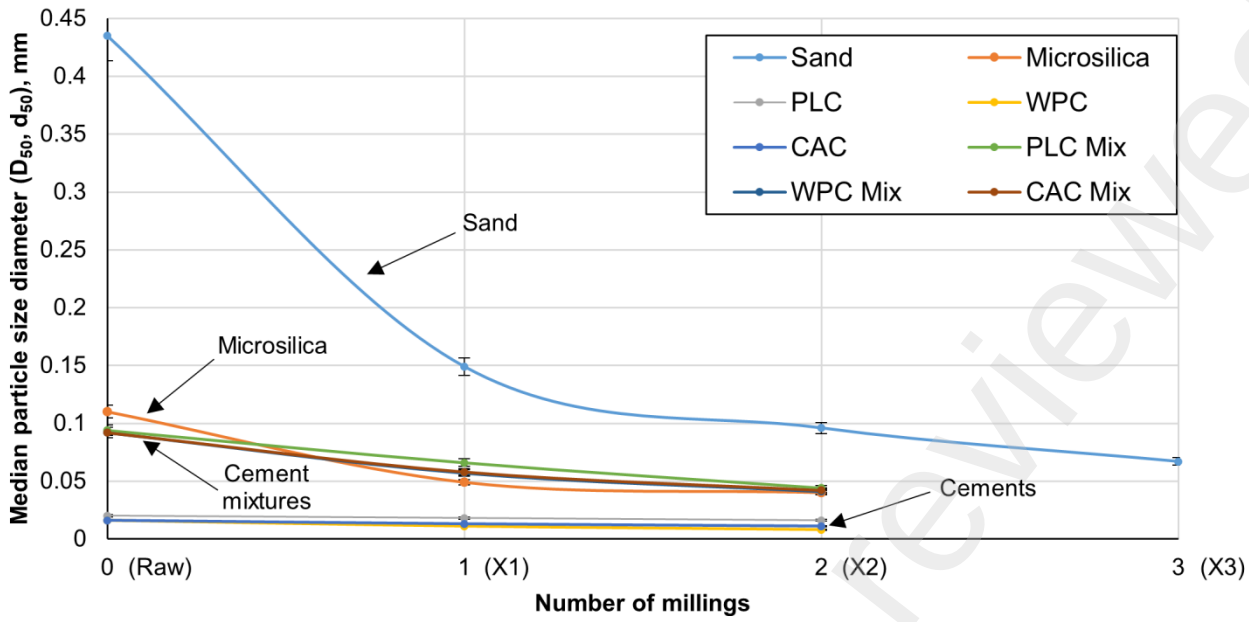

Figure 7. The effect of a milling stage on median particle size diameter (D50, d50). Arrows indicate the distinct results for sand, micro silica, a set of similar results for cement and a set of matching results for cement mixtures with sand and micro silica.

3.3 Effects of milling stages and storage time of cement mixtures on mechanical properties of cement mortars

The effect of the number of milling, day of storing, and the type of cement on the compressive strength measurement results of 3, 7, 14, 28, and 56 days aged PLC, WPC, and CAC based mortar samples are shown in Figure 8 a, b, and c, respectively.

The X1 gives no effect on the early stage of curing (up to 7-days) generated compressive strength of PLC based mortar samples regardless of immediately applied or 3-days long stored milled mixtures, as demonstrated in Figure 8 a. X2 leads up to 29% higher 3-day compressive strength (about 58 MPa) compared to PLC-NM and PLC-X1 samples (about 45 MPa), around 13% higher 7-day compressive strength than PLC-NM samples. The increased reactivity of more fine cementing particles can explain this effect. However, the compressive strength of 28-day cured PLC-NM mortar evolves up to 104 MPa, indicating 20% to 80% higher compressive strength values compared to 28-day aged PLC3-X2 and PLC3-X1 samples, respectively. Further compressive strength development is less intense, with the PLC-NM sample reaching approximately 107 MPa after 56 days of ageing. The higher strength of PLC-NM can be explained by the reinforcement effect of Sand Raw particle sizes [59], more beneficial particle size distribution in the concrete structure, and possibly more beneficial relation of applied constant concentrations of water and superplasticizer to the lower surface area of PLC Raw reactive components, as compared to mortar samples made of PLC Mix X1 and PLC Mix X2. The compressive strength evolvement tendency of PLC-based mixtures becomes similar after 28 days of ageing. However, the PLC0-X1 sample performs a more rapid compressive strength development than PLC0-X2. Therefore, a more extended ageing period is required to estimate the possible final compressive strength value, after which the curve becomes horizontal. The higher the finesse, the higher the reactivity for both cementitious and pozzolanic addition: it means that more time is needed to have the complete activation of all binding components [60].

Generally, the immediate use of X1 and X2 WPC containing mixtures and X2 WPC containing mixture after 3-days storage in the production of mortar leads to an increase in earlier (3-days) compressive strength of mortars by up to about 17 % (WPC3-X2), as compared to WPC-NM, shown in Figure 8 b.

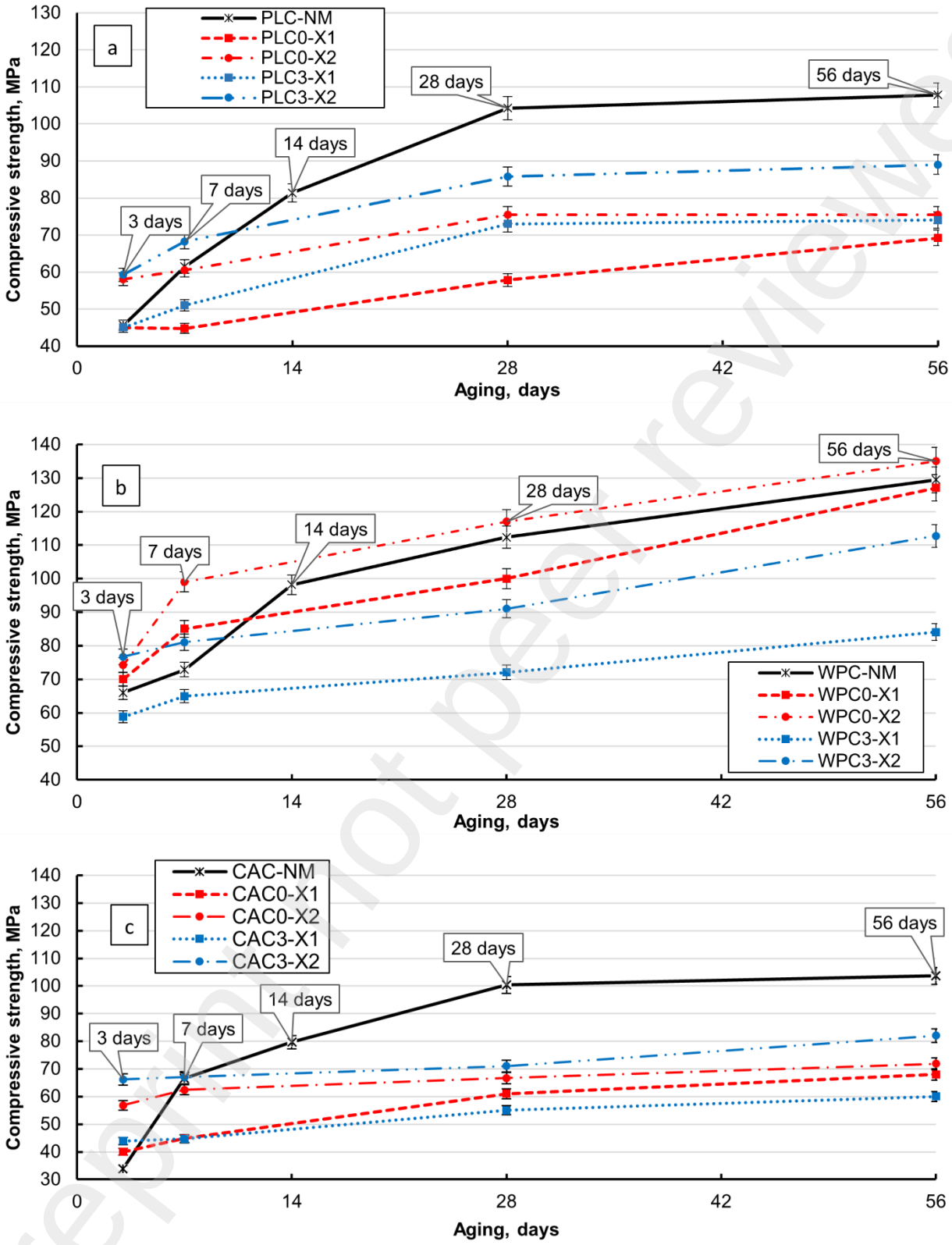

Figure 8. Influence of milling stages and cement type on cured cement mortar compressive strength: NM, X1, and X2 mixtures in compositions with PLC (a), WPC (b), and CAC (c).

However, the use of 3 days stored X2 mixtures causes slower compressive strength development in WPC3-X2 mortar and by about 15 to 22 % lower measured final compressive strength (up to 111 MPa after 56 days) during remaining applied mortar ageing period, as compared to WPC0-X1 (128 MPa), WPC0-X2 (132 MPa), and WPC-NM (135 MPa) specimens. The WPC3-X1 exhibited the lowest compressive strength during the tested ageing period (83 MPa after 56 days). The possible partial hydration of activated WPC particles by the moisture from the air during storage of X1 mixtures and the lower finesse than the X2 can explain this effect. However, the compressive strength development tendency is similar to that detected of immediately used material, and the applied activation approach leads to less observable impact than cases of other tested cement.

X1 and X2 of CAC containing mixtures lead from 1.5 (CAC0-X1, CAC3-X1) up to about two times (CAC0-X2, CAC3-X2) higher earlier (3 days) compressive strength, as compared to the result of CAC-NM (34 MPa), as demonstrated in Figure 8 c. This effect can be explained by higher earlier hydration reaction rate [61] of milled cement particles which results in lower development of compressive strength during further ageing by maintaining about the same trend in the graph, as compared to CAC-NM mortar specimen. The cured CAC-X2 mortar specimen exhibits a rapid increase in 3-day compressive strength up to about 58 MPa, which is relatively close to the final value (72 MPa after 56 days) detected in the range of applied testing conditions. Similar compressive strength development was observed in the case of cured CAC3-X2 specimens, exhibiting 66 MPa to 82 MPa after 3- and 56 days, respectively.

The effect of the applied activation approach on apparent density measurement results of hardened PLC, WPC, and CAC-based mortar samples is shown in Figure 9. All produced PLC based solid mortars exhibited the lowest apparent densities compared to WPC and CAC based specimens made under the same applied conditions.

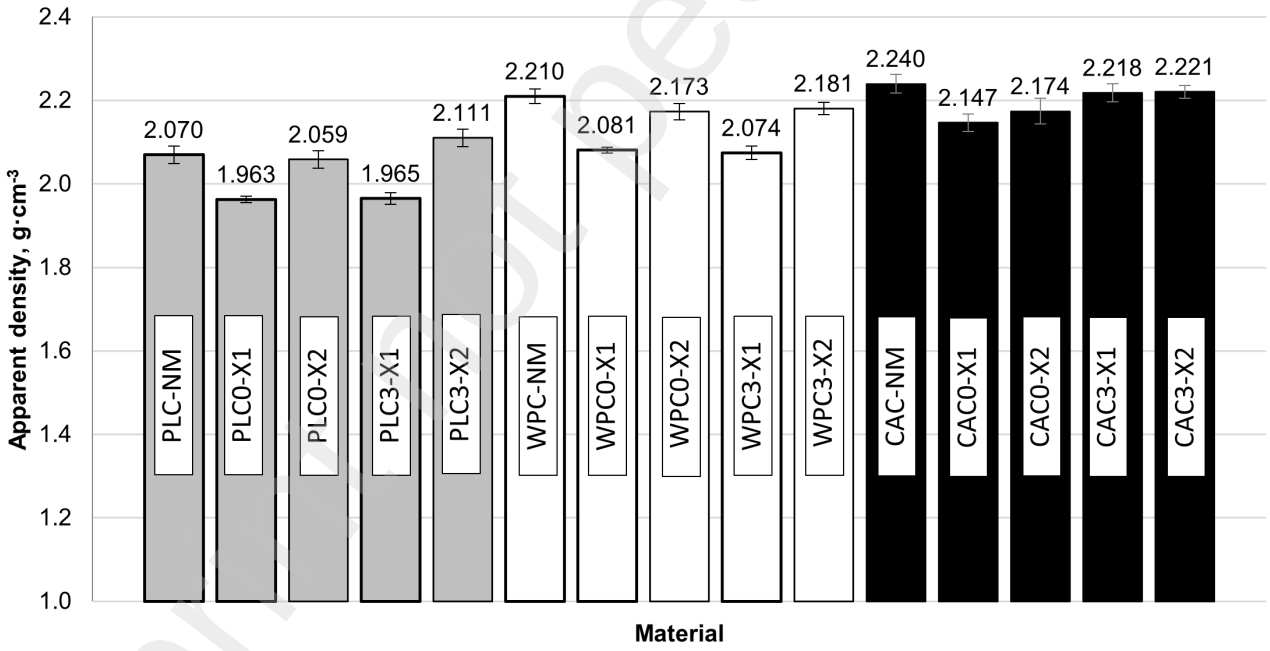

Figure 9. The effect of applied NM, immediately (0 days) and three days stored X1 and X2 mixtures on apparent densities of hardened solid mortars in composition with PLC, WPC, and CAC.

X1 with subsequent immediate use or three days storage of PLC containing dry mixtures leads to a decrease in apparent densities by about 5% from 2.07 g·cm^{-3} (PLC-NM) down to 1.96 g·cm^{-3} (PLC0-X1 and PLC3-X1). This effect can be explained by the less beneficial particle size distribution (loss of coarser sand particles with reinforcing impact) [59] and unadjusted concentrations of superplasticizer and water to the fresh mortar, therefore causing the formation of higher porosity. This type of material cannot be expected as suitable for subjection to

high wear and abrasion conditions [62]. Hardened PLC mortars made of X2 mixtures exhibit similar apparent densities with 0.5 up to 2% differences from PLC-NM mortar due to higher packing densities of finer particles. The presence of fine particles helps to occupy the spaces between larger particles, enhancing the packing density and decreasing the volume of voids that need to be filled with cement paste [63]. A similar trend was observed in the case of WPC-based solid mortars, but with slightly higher apparent density values, as compared to PLC mortar cases.

However, the apparent densities of CAC based hardened solid mortars can be related to differences in activities caused by milling and subsequent storage. Immediately used X1 and X2 mixtures caused high earlier strength (Figure 8 c) indicates the possible higher hydration rate caused a loss in apparent densities by about 3.5 % from 2.24 $g \cdot cm^{-3}$ (CAC-NM) down to about 2.15 $g \cdot cm^{-3}$ (CAC0-X1) and 2.17 $g \cdot cm^{-3}$ (CAC0-X2). The 3-day X1 and X2 mixtures storage led to higher final apparent densities (about 2.2 $g \cdot cm^{-3}$) of hardened CAC mortars compared to cases when X1 and X2 components were used immediately.

In conclusion, the study demonstrates a significant correlation between the apparent densities of produced cement mortars and their measured densities, highlighting the predictive accuracy of apparent density measurements in evaluating mortar characteristics.

3.4 Effect of immediately used and three days stored single-milled PLC- and WPC-based mixtures on mechanical properties of foamed concrete

The dependence of hardened foamed concrete compressive strength on X1 PLC and WPC containing mixtures storing durations (0 and 3 days) after 7-, 28-, and 56-days foamed concrete ageing are demonstrated in Figure 10. It should be noted that all attempts to foam the CAC-containing mixtures with the selected approach failed due to the instability of generated pores and required different approaches, conditions, and additives during further research activities.

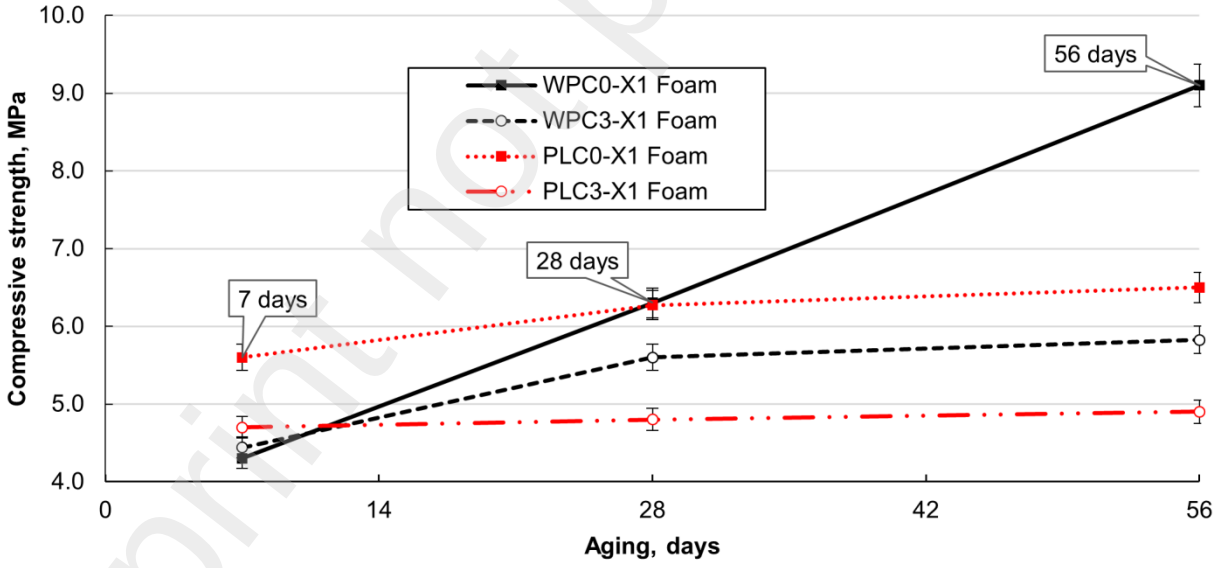

Figure 10. Dependence of foamed concrete compressive strength on X1 PLC and WPC containing mixtures storing durations (0 and 3 days) after 7, 28, and 56 days of ageing.

The 56-day cured PLC0-X1 Foam displayed a compressive strength of 6.53 MPa and an apparent density of 0.996 $g \cdot cm^{-3}$. The WPC0-X1 Foam demonstrated a higher compressive strength of 9.95 MPa but a lower density of 0.915 $g \cdot cm^{-3}$, as demonstrated in Figure 11. Conversely, when the milled mixtures were stored for three days before use, a notable decrease in both compressive strength and apparent density was observed for both types of

foamed concrete. The PLC3-X1 Foam showed a compressive strength of 5.20 MPa and a density of 0.942 g·cm^{-3}, whereas the WPC3-X1 Foam had a compressive strength of 6.63 MPa and a density of 0.879 g·cm^{-3}. This effect represents a 20.37% decrease in compressive strength and a 5.42% decrease in density of foamed concrete made of the PLC-based mixture series, and a more pronounced 33.37% reduction in strength and 3.93% drop in density for the WPC-based mixture series after the 3-days storage period. These results indicate that the storage of milled mixtures, even for a relatively short period, adversely affects the quality of the foamed concrete, underscoring the importance of immediate mixture use after milling in concrete production.

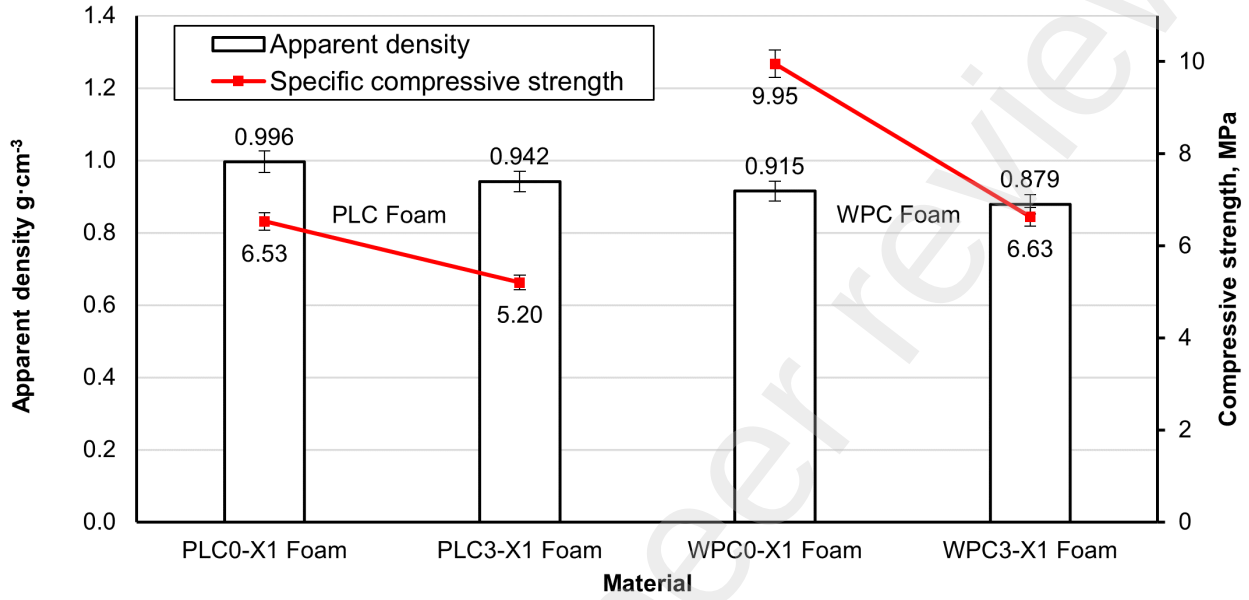

Figure 11. Apparent density and compressive strength dependence on immediate (0 days) and three days storing before use in the manufacturing of X1 and subsequently foamed PLC and WPC concrete after 56 days of curing.

3.5 Effects of milling stages and storage time of cement mixtures on morphologies of cement mortars and foamed concrete

The visual impact of X1 and X2 on the microstructures of cement mortars after 56 days of ageing is depicted in Figure 12. In comparison to NM mortar samples, both X1 and X2 samples displayed the presence of finer particles.

The NM mortar samples contained visible sand particles with sizes reaching up to 300 µm (PLC0-NM) and 500 µm (WPC0-NM and CAC0-NM), consistent with the particle size analysis results shown in Figure 6. Remarkably, no significant differences in particle sizes were observed between the X1 and X2 samples, as evidenced in Figure 12 b, c, e, f, h, and g. These mortar specimens exhibited observable particle sizes ranging from 50 to 150 µm.

While there appeared to be a slightly larger particle size on the surface of PLC0-X2 (Figure 12 c) cement mortar compared to PLC0-X1 (Figure 12 b), this discrepancy can be considered coincidental. Upon conducting a more extensive microscopic analysis, this difference disappeared. It is worth noting that cement mortars created from dry mixtures stored for three days exhibited similar visually observable particle sizes.

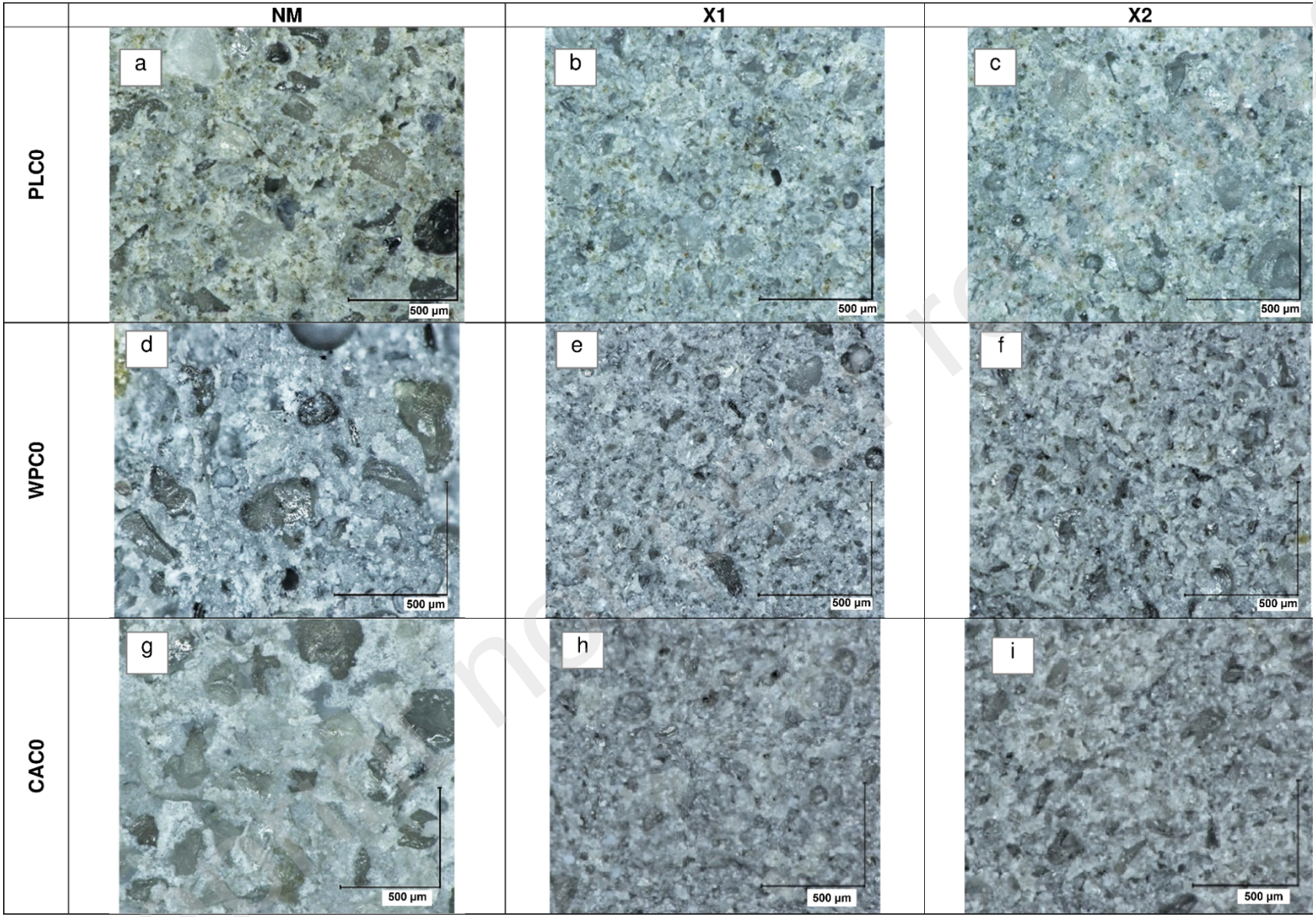

Figure 12. Detailed optical microscopy images (X50 magnification) of fractured cement mortar specimens after 56-day hardening made of (a) NM PLC, (b) X1 PLC, (c) X2 PLC, (d) NM WPC, (e) X1 WPC, (f) X2 WPC, (g) NM CAC, (h) X1 CAC, (i) X2 CAC based samples.

Figure 13 illustrates visually observable pores at fracture sites in foamed concrete samples based on PLC and WPC produced from 3-day stored dry mixtures.

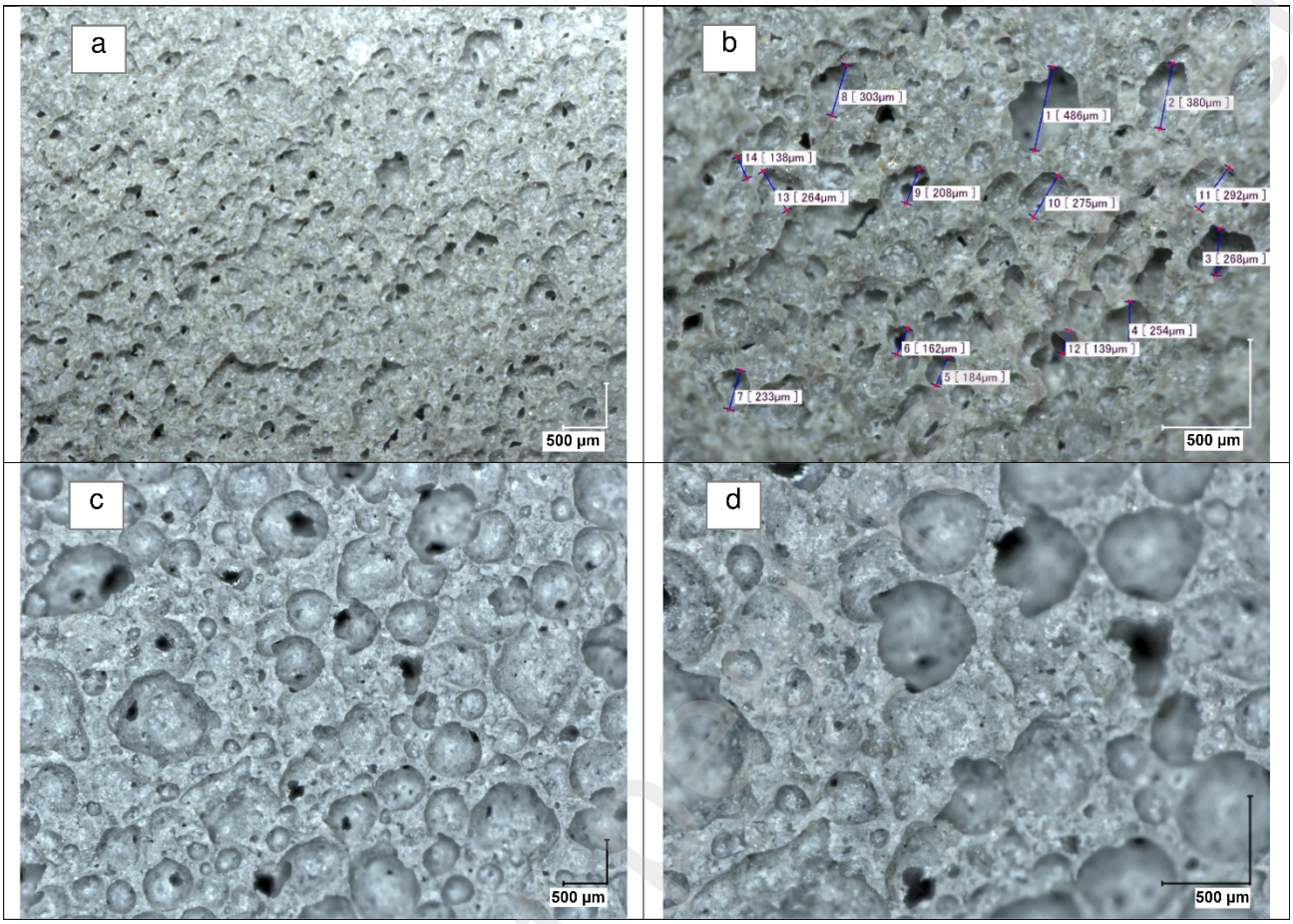

Figure 13. Optical microscopy images of 56-days cured PLC3-X1 Foam (a - X50 and b - X100 magnification) and WPC3-X1 Foam (c - X50 and d - X100 magnification).

In the case of the PLC3—X1 Foam sample, there is a more consistent distribution of pore sizes, primarily ranging from 138 µm to 480 µm. On the other hand, the WPC3—X1 Foam sample displays a broader spectrum of pore sizes, spanning approximately 100 to 1000 µm. Furthermore, the WPC3—X1 Foam matrix exhibits a visibly higher density of larger pores ranging from 500 to about 1000 µm, which are also more rounded in shape than the PLC3—X1 Foam, as depicted in Figure 13 b and d. Similar pores were observed on the surfaces of WPC0-X1 Foam samples. The PLC0-X1 Foam samples notably generated slightly more prominent pores, with sizes reaching up to 532 µm, as shown in Figure 14, in contrast to the PLC3-X1 Foam samples, illustrated in Figure 13 a and b.

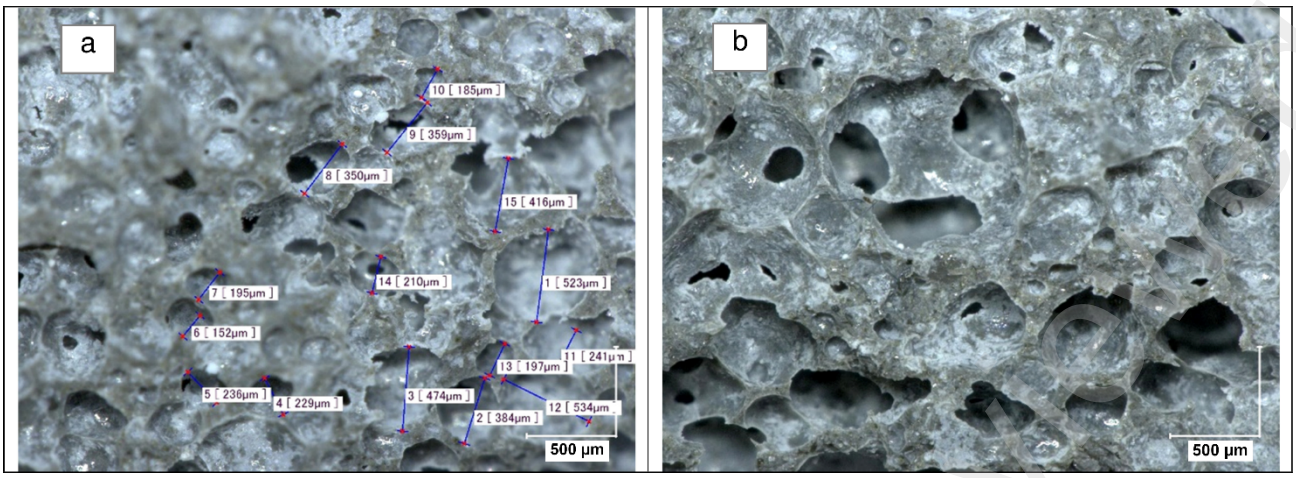

Figure 14. Optical microscopy images of 56-days cured PLC0—X1 Foam (a - X50 and b - X100 magnification).

4. DISCUSSION

The foamed concrete produced in this study, aged for 56 days and with densities ranging from 0.879 g·cm^{-3} (WPC3-X1 Foam) to 0.996 g·cm^{-3} (as illustrated in Figure 11), meets the classification criteria for foam concrete as defined in references [4,5]. These density values are notably higher than the American Society for Testing and Materials (ASTM) requirements in standard C869/C869M – 11 [64]. This standard specifies an oven-dry density for cellular concrete ranging from 0.47 g·cm^{-3} (±0.04 g·cm^{-3}) to 0.49 g·cm^{-3} (±0.04 g·cm^{-3}) for type I and type III cements, respectively. It is also significant to mention that the compressive strength of the produced foamed concrete, ranging from 5.20 to 9.95 MPa (Figure 11), substantially surpasses the minimum required compressive strength of 1.4 MPa as stipulated in ASTM C869/C869M – 11 [64]. For further investigations, it is imperative to comprehensively assess the operational parameters of the equipment, such as rotation speed and working temperature, for both the disintegrator and HSMD. Additionally, the performance of other essential components within the innovative production system, including containers, pipelines, and mixers, should be thoroughly evaluated. This evaluation aims to optimize the production process for cement mortar and foam concrete, ensuring that the resulting properties meet industry requirements and provide the necessary level of repeatability. In future studies, it is essential to evaluate the permeability of water, corrosive substances, and gases, and the resistance to freeze-thaw cycles of cement mortar and foam concrete produced using this innovative technique.

The primary cementitious material utilized in manufacturing foamed concrete is traditional Portland cement, valued for its high strength, minimal dry shrinkage, and durability. However, the cement industry is responsible for approximately 8% of global anthropogenic CO_2 emissions, respectively [65]. The excessive extraction of sand and gravel severely threatens the stability of river channels and ecosystems [66]. This process hampers the sustainability of foamed concrete and contributes to environmental degradation. Therefore, it is necessary to develop an alternative cement or partially substituted cement-based solution for foamed concrete production. The failure to produce foamed concrete with the selected foaming agent from CAC in the present study prompts a range expansion of possible foaming agents. There needs to be more information in the literature on the direct use of foaming agents in producing CAC-based concrete foams. However, there is information on efforts and results using CAC analogue cement.

One of the examples is the role of protein-based surfactants in producing non-autoclaved bio-based foamed concretes. Key findings include hemp shives increasing the porosity but reducing mechanical strength, while cement and pozzolanic materials enhance pore uniformity and compressive strength. The production method significantly affects pore formation, with the preformed method being more effective for lightweight concrete. Mechanical strength largely depends on porosity, mineral matrix strength, pore distribution and size [67].

Another study investigated the formulation of foamed concrete using sulphate aluminium cement, fly ash, H_2O_2, $FeCl_3$, calcium stearate, and $Ce(SO_4)_2 \cdot 4H_2O$. Authors have explored replacing cement with fly ash (up to 20% by weight), using H_2O_2 and $FeCl_3$ as foaming agents and $Ce(SO_4)_2 \cdot 4H_2O$ as an additive. The examination focused on the effects of these components on the density and compressive strength of the concrete. It has been found that Ce^{4+} enhances foam stability, reduces foaming time, improves foaming ability, and significantly lowers the dry density of the foamed concrete, achieving a density of 0.22-0.32 $g \cdot cm^{-3}$ and compressive strength of 0.2-0.65 MPa [68].

In subsequent research, various approaches should be explored for preparing dry raw material mixtures to prevent the excessive concentration of fine particles. These fine particles increase the total surface area of solid particles, leading to excessive water absorption and the need for increased concentration of expensive superplasticizers to achieve flowable cement mortar paste [69]. Currently, the cheapest plasticizers are lignosulphonates-based surfactants with typical consumption of 0.15–0.25% by cement weight [70]. Plasticizers significantly improve the workability of foam concrete mixtures, particularly those with 63–80% foam content [71]. They reduce stress on the concrete's pores, ensuring smoother cement slurry flow and more uniform distribution within the pores. This uniformity prevents pore merging and increases pore size, enhancing the foam concrete's structure and stability [72]. A higher pore count means more pore walls. Also, as the density of the foamed concrete paste rises, the peak frequency distribution of pore wall thickness tends to decrease [73]. Total granulometric composition shifting toward small particles also results in an undesirably low packing density of concrete pore walls [74] causing wall effects between particles when foamed concrete is subjected to mechanical loads. The wall effect occurs when coarse particles in a mixture predominantly made of fine powder displace the finer ones. If these coarse particles are not sizable enough to fill the spaces, they create voids instead [75]. To address this effect, one should consider adopting a different composition for the initial cement-sand-microsilica mixture that will undergo grinding in the disintegrator. The remaining Sand Raw and other reinforcing aggregates can be added during subsequent mixing of dry aggregates to obtain the cement mortar paste or during the treatment of the paste with the HSMD, with mixing taking place in the working chamber of the disperser. This approach will result in an adapted granulometric composition of solid particles, significantly influencing the packing density and overall performance of the cement mortar and foam concrete matrix.

The energy consumption for milling can be tailored through the services offered by commercial concrete raw material manufacturers, leveraging their extensive range of products to achieve a custom granulometric composition with the desired admixture activity. For instance, the microsilica Grade 92D (densified) utilized in this study is also available as Grade 92U (undensified) [76]. Nonetheless, it is essential to consider the impact of transportation and storage duration on the activity and reagglomeration of filler particles, as these factors significantly influence the properties of cement mortar and foam concrete.

For scaling (industrialization) purposes, it is also crucial to estimate equipment depreciation and operating costs for the entire production scheme, considering the aggregates involved. The recently developed industrial-scaled disintegrators offer three milling systems: direct, separative (closed), and selective, catering to diverse processing needs such as testing material properties, producing materials with varied granularity, and processing in dry, wet, or liquid forms, with additional capabilities like mixing and drying [77]. Direct milling setup processes the material through high intensity impacts in a single pass to the collector, suitable for a broad range of applications, including testing and producing materials with wide granularity. Separative milling achieves the desired fineness by employing a classifier method to process the material repeatedly. Selective milling, meanwhile, separates materials based on density or strength and is used to refine components of multicomponent materials or extract valuable elements from industrial waste, ensuring minimal impact on other components [78].

It is worth noting that this innovative production scheme can be adapted for both factory-based production and on-site production of cement mortar and foam concrete. It is imperative to conduct meticulous measurements of

the feed rate of dry particles for the disintegrator and the flow rate of cement mortar paste for the HSMD to achieve more precise energy consumption calculations.

Additionally, expanding the innovative production scheme (see Figure 2) to include the capability of producing cement mortar using the HSMD without utilizing the foaming function is crucial. The hydrodynamic cavitation without gases (e.g., O_2, O_3, CO_2) [79] may lead to improved workability caused by water vapours in cavities. Such an approach would enable a more objective comparison of the properties of cement mortars and foam concrete under similar manufacturing conditions. Furthermore, additional research is warranted to assess the potential of the innovative production scheme and the advanced equipment it incorporates, namely the disintegrator and HSMD, in manufacturing cement mortar and foam concrete using recycled concrete aggregates [80].

5. CONCLUSIONS

The analysis yields significant insights into milling (with the help of two rotor disintegrator model DSL-115) process efficacy, particle size reduction, and energy consumption, with notable numerical values to support these conclusions. Raw sand's median particle size, initially at 0.435 mm ($D_{50\_Sand\ Raw}$), decreased significantly to 0.067 mm ($D_{50\_Sand\ X3}$) after X3, while PLC's median particle size reduced from 0.020 mm ($D_{50\_PLC\ Raw}$) to 0.016 mm ($d_{50\_PLC\ X2}$) following X2. Similar reductions in particle sizes were observed for components like WPC and CAC.

The degree of milling exhibited variations among components. For instance, sand showed the highest degree at 4.54 after X2 and 6.52 after X3. In contrast, components like PLC and WPC had lower degrees of milling, with values ranging from 1.09 (PLC X1) to 1.97 (WPC X2).

Energy consumption played a crucial role, with clear numerical distinctions. Milling sand's energy requirement doubled from 4.3 $kW{\cdot}h{\cdot}T^{-1}$ (Sand X1) to 8.6 $kW{\cdot}h{\cdot}T^{-1}$ (Sand X2). Cement-sand-microsilica mixtures required an additional 2.15 $kW{\cdot}h{\cdot}T^{-1}$ for mixing without milling, highlighting the initial energy investment even before milling. This consistent increase in energy consumption was a common trend across all components and mixtures studied.

Due to milling processes, the granulometric analysis of raw and milled sand and microsilica reveals significant alterations in particle size distribution, particularly in the finer range. This finding, combined with the critical role of particle size in cement mortar's compressive strength, underscores the superiority of X1 mixtures for producing foamed cement samples with optimal performance characteristics.

In the context of foamed concrete (produced with the help of HSMD model KMD 1,5), the influence of milling processes and material storage on compressive strength, apparent density, and microstructure is evident, with crucial numerical data to support these findings. However, it is essential to note that the attempts to produce foam from CAC-containing mixtures with the selected approach were unsuccessful, indicating the need for alternative methods, conditions, and additives in future research.

Immediate utilization of X1 and X2 PLC and WPC-containing mixtures increased 3-day compressive strength. For instance, the PLC0-X1 Foam exhibited a compressive strength of 6.53 MPa, while the WPC0-X1 Foam demonstrated a higher compressive strength of 9.95 MPa. Conversely, storing milled mixtures for three days led to a notable decrease in compressive strength and apparent density. The PLC3-X1 Foam displayed a compressive strength of 5.20 MPa, whereas the WPC3-X1 Foam had a compressive strength of 6.63 MPa, representing a 20.37% and 33.37% reduction, respectively. These numerical values underscore the adverse impact of material storage on foam concrete quality, highlighting the significance of immediate material use after milling in concrete production.

The PLC3—X1 Foam sample exhibits a consistent and uniform pore size distribution, primarily ranging from 138 μm to 480 μm, indicating a more uniform cellular structure. In contrast, the WPC3—X1 Foam sample shows

a broader spectrum of pore sizes from approximately 100 μm to 1000 μm, with a higher density of larger, more rounded pores between 500 μm to about 1000 μm. This result suggests a more heterogeneous pore distribution within the WPC3—X1 Foam. Additionally, similar large pores are observed in WPC0-X1 Foam samples, while PLC0-X1 Foam samples generate slightly larger pores than PLC3—X1 Foam, reaching up to 532 μm. These characteristics suggest significant differences in microstructural properties between PLC and WPC mixtures based foamed concrete series, potentially affecting their application performance based on pore size and distribution.

CRediT authorship contribution statement

Janis Baronins, Andrei Shishkin, Vitalijs Lusis, Dmitri Goljandin: Conceptualization, Investigation. Janis Baronins, Andrei Shishkin, Chiara Giosuè, Pavels Gavrilovs: Visualization, Writing – original draft. Janis Baronins, Andrei Shishkin, Aleksandrs Korjakins, Dmitrijs Gorelikovs, Iveta Novakova, Sofija Kekez: Funding acquisition, Writing – review & editing. Andrei Shishkin, Vitalijs Lusis: Methodology, Resources. Janis Baronins, Andrei Shishkin: Supervision. Janis Baronins, Andrei Shishkin, Iveta Novakova: Data curation, Iveta Novakova: Project administration.

Declaration of competing interest

The authors declare that they have no conflict of interest.

Data availability

Data will be made available on request.

Funding

This research was funded by Interreg Northern Periphery and Arctic programme 2021-2027 [Project No. NPA0100039, Ar2CorD]. The article was published with financial support from the Riga Technical University Research Support Fund.

Acknowledgements

We express our heartfelt appreciation to the Interreg Bridging Call Project Ar2CorD for their invaluable support during the crucial stages of final analysis and drafting of this study. We also extend our sincere thanks to the dedicated team at Building Materials: Design-Testing-Application (DeTeA) within the Department of Building, Energy, and Material Technology at UiT The Arctic University of Norway. Their expert assistance in data analysis and contributions to the drafting of the final thesis were instrumental to our research. Furthermore, this work was made possible through the support of the Estonian Research Council grant [Project No PRG643], which facilitated the milling and sieving analysis of raw materials, contributing significantly to our findings.

REFERENCES

[1] Liu X, Ni C, Meng K, Zhang L, Liu D, Sun L. Strengthening mechanism of lightweight cellular concrete filled with fly ash. Constr Build Mater 2020;251:118954. https://doi.org/10.1016/j.conbuildmat.2020.118954.

[2] Deni N, Gladstone RA. Low-density cellular concrete in MSE structures with steel strip reinforcements—design and construction considerations and case histories. Geo-Congress 2019, Reston, VA: American Society of Civil Engineers; 2019, p. 127–39. https://doi.org/10.1061/9780784482087.012.

[3] Davies DR, Hartog JJ, Cobbett JS. Foamed cement - A cement with many applications. Middle East Technical Conference and Exhibition, Society of Petroleum Engineers; 1981, p. 15. https://doi.org/10.2118/9598-MS.

[4] Tanveer, A., Jagdeesh, K., Ahmed F. Foam concrete. International Journal of Civil Engineering Research 2017;8:1–14.

[5] Tan X, Chen W, Hao Y, Wang X. Experimental study of ultralight (<300 kg/m3) foamed concrete. Advances in Materials Science and Engineering 2014;2014. https://doi.org/10.1155/2014/514759.

[6] Legatski L. Cellular concrete. Significance of tests and properties of concrete and concrete-making materials, vol. 1, West Conshohocken: ASTM International; 1978, p. 836–51. https://doi.org/10.1520/STP35648S.

[7] Li T, Wang Z, Zhou T, He Y, Huang F. Preparation and properties of magnesium phosphate cement foam concrete with H2O2 as foaming agent. Constr Build Mater 2019;205:566–73. https://doi.org/10.1016/J.CONBUILDMAT.2019.02.022.

[8] Mohd Zamzani N, Othuman Mydin MA, Abdul Ghani AN. Mathematical regression models for prediction of durability properties of foamed concrete with the inclusion of coir fibre. Int J Eng Adv Technol 2019;8:3353–8. https://doi.org/10.35940/ijeat.F9502.088619.

[9] Kearsley EP, Wainwright PJ. The effect of porosity on the strength of foamed concrete. Cem Concr Res 2002;32:233–9. https://doi.org/10.1016/S0008-8846(01)00665-2.

[10] Sugama T, Brothers LE, de Putte TR Van. Air-foamed calcium aluminate phosphate cement for geothermal wells. Cem Concr Compos 2005;27:758–68. https://doi.org/10.1016/j.cemconcomp.2004.11.003.

[11] Rudolph C. Valore Jr. Cellular concretes. Part 2 - Physical properties. ACI Journal Proceedings, vol. 50, 1954, p. 817–36. https://doi.org/10.14359/11795.

[12] Studart AR, Innocentini MDM, Oliveira IR, Pandolfelli VC. Reaction of aluminum powder with water in cement-containing refractory castables. J Eur Ceram Soc 2005;25:3135–43. https://doi.org/10.1016/j.jeurceramsoc.2004.07.004.

[13] Baronins J, Shishkin A, Setina J, Mironovs V. Influence of Al-W-B recycled composite material on the properties of high performance concrete. Construction Science 2015;17. https://doi.org/10.1515/cons-2015-0001.

[14] Gökçe HS, Hatungimana D, Ramyar K. Effect of fly ash and silica fume on hardened properties of foam concrete. Constr Build Mater 2019;194:1–11. https://doi.org/10.1016/J.CONBUILDMAT.2018.11.036.

[15] Namsone E, Korjakins A, Sahmenko G, Sinka M. The environmental impacts of foamed concrete production and exploitation. IOP Conf Ser Mater Sci Eng 2017;251:012029. https://doi.org/10.1088/1757-899X/251/1/012029.

[16] Yang S, Wang X, Hu Z, Li J, Yao X, Zhang C, et al. Recent advances in sustainable lightweight foamed concrete incorporating recycled waste and byproducts: A review. Constr Build Mater 2023;403:133083. https://doi.org/10.1016/j.conbuildmat.2023.133083.

[17] T. Ergene M. Method for forming foamed concrete structures. 3,758,319, 1973.

[18] Hwang C-L, Tran V-A. A study of the properties of foamed lightweight aggregate for self-consolidating concrete. Constr Build Mater 2015;87:78–85. https://doi.org/10.1016/J.CONBUILDMAT.2015.03.108.

[19] Birzniece IM, Cizevska A, Goljandin D, Lusis V. Comparison of electrical conductivity of cement composite materials, 2023, p. 080011. https://doi.org/10.1063/5.0170574.

[20] Vinarov A, Sokolov D, Sokolova E, Panteleev V. Method of producing foam concrete using a protein foamer. WO1999062842A1, 1998.

[21] Jiang J, Lu Z, Niu Y, Li J, Zhang Y. Study on the preparation and properties of high-porosity foamed concretes based on ordinary Portland cement. Mater Des 2016;92:949–59. https://doi.org/10.1016/j.matdes.2015.12.068.

[22] Kim D. Effect of adjusting for particle-size distribution of cement on strength development of concrete. Advances in Materials Science and Engineering 2018;2018:1–6. https://doi.org/10.1155/2018/1763524.

[23] Alekseevich Efimov P, Alekseevich Efimov A, Petrovich P, Petrovich Pustovgar A. Dry mortar for preparation of cellular concrete. RU2392245C1, 2008.

[24] Justs J., Shakhmeno G., Mironovs V. KP. Cavitation treatment of nano and micro filler and its effect on the properties of UHPC. Proceedings of Hipermat 2012 3rd Inernational Symposium on UHPC and Nanotechnology for High Performance Construction Materials 2012;19:87–92.

[25] Denis Robertovich S. A new method for producing foam concrete and homogeneous systems in a turbulent cavitation type mixer (in Russian). Construction Materials, Equipment, Technologies of the 21st Century 2004;12:38–40.

[26] Just A, Middendorf B. Microstructure of high-strength foam concrete. Mater Charact 2009;60:741–748. https://doi.org/10.1016/j.matchar.2008.12.011.

[27] Baronins J, Setina J, Sahmenko G, Lagzdina S, Shishkin A. Pore distribution and water uptake in a cenosphere-cement paste composite material. IOP Conf Ser Mater Sci Eng, vol. 96, 2015. https://doi.org/10.1088/1757-899X/96/1/012011.

[28] Polyakov A, Polykova E. Mixer-Disperser. DE202007014913.1, 2007.

[29] Kosmatka SH. Fly ash, slag, silica fume, and natural pozzolans. Design and control of concrete mixtures. 7th ed., Paris: Cement Association of Canada; 2002, p. 57–72.

[30] Rixom MR, Mailvaganam NP. Chemical admixture for concrete. 2nd edition. London: Spon Press; 1986.

[31] Legrand C, Wirquin E. Effects of the initial structure of the cement paste in fresh concrete on the first development of strength. Communication Papers Theme IV, Proceedings of an International Conference, New Delhi: NCB,; 1992, p. 95–101.

[32] Andersen PJ, Roy DM, Gaidis JM, W.R. Grace & Co. The effects of adsorption of superplasticizers on the surface of cement. Cem Concr Res 1987;17:805–13. https://doi.org/10.1016/0008-8846(87)90043-3.

[33] Foisy A, Persello J. Surface group ionization un silicas. In: Legrand AP, editor. The Surface Properties of Silicas. 1st edditi, Hoboken: Wiley; 1998, p. 365–414.

[34] Chandra S, Ohama Y. Polymers in concrete. 1st edition. Boca Raton: CRC Press; 1994.

[35] Hewlett PC. Lea's chemistry of cement and concrete. 4th edition. Elsevier; 2003. https://doi.org/10.1016/B978-0-7506-6256-7.X5007-3.

[36] Bakalejnik GKh, Ivanitskij V V., Gonchar VF, Buryanov AF, Stepanenko V V., Lychakov VI, et al. Mixer (in Russian). SU1694395A1, 1989.

[37] Krauss Juillerat F, Gonzenbach UT, Elser P, Studart AR, Gauckler LJ. Microstructural control of self-setting particle-stabilized ceramic foams. Journal of the American Ceramic Society 2011;94:77–83. https://doi.org/10.1111/j.1551-2916.2010.04040.x.

[38] Krauss Juillerat F, Gonzenbach UT, Gauckler LJ. Tailoring the hierarchical pore structures in self-setting particle-stabilized foams made from calcium aluminate cement. Mater Lett 2012;70:152–4. https://doi.org/10.1016/j.matlet.2011.12.006.

[39] Gonzenbach UT, Studart AR, Tervoort E, Gauckler LJ. Stabilization of foams with inorganic colloidal particles. Langmuir 2006;22:10983–8. https://doi.org/10.1021/la061825a.

[40] Binks BP. Particles as surfactants—similarities and differences. Curr Opin Colloid Interface Sci 2002;7:21–41. https://doi.org/10.1016/S1359-0294(02)00008-0.

[41] Gonzenbach UT, Studart AR, Tervoort E, Gauckler LJ. Ultrastable particle-stabilized foams. Angewandte Chemie 2006;118:3606–10. https://doi.org/10.1002/ange.200503676.

[42] Bushnell-Watson SM, Sharp JH. The effect of temperature upon the setting behaviour of refractory calcium aluminate cements. Cem Concr Res 1986;16:875–84. https://doi.org/10.1016/0008-8846(86)90011-6.

[43] Siskins A, Korjakins A, Bajare D, Sahmenko G, Namsone E. Method of manufacturing fine-grained foam concrete using two-stage activation: mechanical and with a cavitation efect. LV15522B, 2020.

[44] Shishkin A, Mironovs V, Vu H, Novak P, Baronins J, Polyakov A, et al. Cavitation-dispersion method for copper cementation from wastewater by iron powder. Metals (Basel) 2018;8:920. https://doi.org/10.3390/met8110920.

[45] SIKA. Sikament® 56 Technical data sheet. Technical Data Sheet 2016:2. http://lva.sika.com/dms/getdocument.get/4aa76c8e-e844-38d4-be34-e3d2d44ab7c2/Sikament-56_lv_c.pdf.

[46] Shishkin A, Korjakins A, Mironovs V. Using of cavitation disperser, for porous ceramic and concrete material preparation. International Journal of Environmental, Chemical, Ecological, Geological and Geophysical Engineering 2015;9:540–3.

[47] GÓRKA CEMENT LTD. GÓRKAL 70 - high alumina cement. Product Description 2017:1–1. http://www.gorka.com.pl/pdf/en/g70_katalog_en.pdf.

[48] Lapkovskis V, Mironovs V, Goljandin D. Suitability of devulcanized crumb rubber for oil spills remediation. Energy Procedia 2018;147:351–7. https://doi.org/10.1016/j.egypro.2018.07.103.

[49] Shishkin A, Baronins J, Mironovs V, Lukáč F, Štubňa I, Ozolins J. Influence of glass additions on illitic clay ceramics. Materials 2020;13:596. https://doi.org/10.3390/ma13030596.

[50] Zhang J, Ke G, Liu Y. Early hydration heat of calcium sulfoaluminate cement with influences of supplementary cementitious materials and water to binder ratio. Materials 2021;14:642. https://doi.org/10.3390/ma14030642.

[51] Bumanis G. Performance evaluation of cement mortar and concrete with incorporated micro fillers obtained by collision milling in disintegrator. Ceramics - Silikaty 2017:231–43. https://doi.org/10.13168/cs.2017.0021.

[52] Kumar A, Sahu R, Tripathy SK. Energy-efficient advanced ultrafine grinding of particles using stirred mills— A review. Energies (Basel) 2023;16:5277. https://doi.org/10.3390/en16145277.

[53] Moon S-W, Vinoth G, Subramanian S, Kim J, Ku T. Effect of fine particles on strength and stiffness of cement treated sand. Granul Matter 2020;22:9. https://doi.org/10.1007/s10035-019-0975-6.

[54] Aydın S, Karatay Ç, Baradan B. The effect of grinding process on mechanical properties and alkali–silica reaction resistance of fly ash incorporated cement mortars. Powder Technol 2010;197:68–72. https://doi.org/10.1016/j.powtec.2009.08.020.

[55] C. Holland T. Silica fume - Users manual. 2nd ed. WASHINGTON: U.S. Dept of Transportation/Federal Highway Administration; 2005.

[56] Sun Z, Liu Y, Shui L, Tang X, Dong Y, Li D. Grey connection analysis between cement particle size distribution and compressive strength. Proceedings of the 2015 International Conference on Architectural, Civil and Hydraulics Engineering, Paris, France: Atlantis Press; 2015. https://doi.org/10.2991/icache-15.2015.12.

[57] Stefanidou M, Koltsou P. The role of sand in mortar's properties. Sand in Construction, IntechOpen; 2022. https://doi.org/10.5772/intechopen.102489.

[58] Matsanga N, Nheta W, Chimwani N. Effects of particle size distribution of standard sands on the physical-mechanical properties of mortars. Minerals 2023;13:1373. https://doi.org/10.3390/min13111373.

[59] Ferreira RLS, Medeiros M, Pereira JES, Henriques GF, Tavares JC, Marvila MT, et al. Effects of particle size distribution of standard sands on the physical-mechanical properties of mortars. Materials 2023;16:844. https://doi.org/10.3390/ma16020844.

[60] Bouaziz A, Hamzaoui R, Guessasma S, Lakhal R, Achoura D, Leklou N. Efficiency of high energy over conventional milling of granulated blast furnace slag powder to improve mechanical performance of slag cement paste. Powder Technol 2017;308:37–46. https://doi.org/10.1016/j.powtec.2016.12.014.

[61] Koňáková D. Thermal resistance of calcium aluminate cement based composites. Doctoral thesis. Czech Technical University in Prague, 2018. https://doi.org/10.2/JQUERY.MIN.JS.

[62] Alaka HA, Oyedele LO, Toriola-Coker OL. Effect of excess dosages of superplasticizer on the properties of highly sustainable high-volume fly ash concrete. International Journal of Sustainable Building Technology and Urban Development 2016;7:73–86. https://doi.org/10.1080/2093761X.2016.1167643.

[63] Kwan AKH, Ng PL, Huen KY. Effects of fines content on packing density of fine aggregate in concrete. Constr Build Mater 2014;61:270–7. https://doi.org/10.1016/j.conbuildmat.2014.03.022.

[64] ASTM. C869/C869M - Standard specification for foaming agents used in making preformed foam for cellular concrete. 2016.

[65] Campo F Pietro, Tua C, Biganzoli L, Pantini S, Grosso M. Natural and enhanced carbonation of lime in its different applications: a review. Environmental Technology Reviews 2021;10:224–37. https://doi.org/10.1080/21622515.2021.1982023.

[66] Zhai W, Ding J, An X, Wang Z. An optimization model of sand and gravel mining quantity considering healthy ecosystem in Yangtze River, China. J Clean Prod 2020;242:118385. https://doi.org/10.1016/j.jclepro.2019.118385.

[67] Mohamad A, Khadraoui F, Chateigner D, Boutouil M. Influence of porous structure of non-autoclaved bio-based foamed concrete on mechanical strength. Buildings 2023;13:2261. https://doi.org/10.3390/buildings13092261.

[68] Jing Z, Xiangdong L. Effect of rare earth Ce4+ content on the properties and form mechanism of foamed concrete. Biotechnol (Rajkot) 2014;10:15573–82.

[69] Wang L, Ma Y, Li L. Uncovering the role of superplasticizer in developing nano-engineered ultra-high-performance concrete. Front Mater 2023;10. https://doi.org/10.3389/fmats.2023.1177189.

[70] Dvorkin L, Zhitkovsky V, Makarenko R, Ribakov Y. The influence of polymer superplasticizers on properties of high-strength concrete based on low-clinker slag portland cement. Materials 2023;16:2075. https://doi.org/10.3390/ma16052075.

[71] Fu Y, Wang X, Wang L, Li Y. Foam concrete: a state-of-the-art and state-of-the-practice review. Advances in Materials Science and Engineering 2020;2020:1–25. https://doi.org/10.1155/2020/6153602.

[72] Bagheri A, Samea SA. Parameters influencing the stability of foamed concrete. Journal of Materials in Civil Engineering 2018;30. https://doi.org/10.1061/(ASCE)MT.1943-5533.0002290.

[73] Chen J, Chen B, Chen X, Qiang S, Zheng Y. Study on pore structure of foamed cement paste by multi-approach synergetics. Constr Build Mater 2023;362:129748. https://doi.org/10.1016/j.conbuildmat.2022.129748.

[74] German RM. Prediction of sintered density for bimodal powder mixtures. Metallurgical Transactions A 1992;23:1455–65. https://doi.org/10.1007/BF02647329.

[75] Abu-Lebdeh TM, Damptey R, Ungureanu LM, Petrescu FIT. A ternary model for particle packing optimization. Journal of Composites Science 2022;6:113. https://doi.org/10.3390/jcs6040113.

[76] Xiamen All Carbon Corporation. Undensified microsilica (silica fume), SiO2, 92% (min) | ACC. Data Sheet 2024:1–1. https://www.allcarbon.info/microsilica/undensified-microsilica-silica-fume-sio2-92-min/ (accessed February 10, 2024).

[77] Siskins A. Research and development of multifunctional porous materials on the basis of clay and glass waste. Doctoral thesis. Riga Technical University, 2021. https://doi.org/10.7250/9789934226335.

[78] Kulu P, Goljandin D. Retreatment of Polymer Wastes by Disintegrator Milling. In: Achilias DS, editor. Waste Material Recycling in the Circular Economy - Challenges and Developments, Thessaloniki: IntechOpen; 2021, p. 1–23. https://doi.org/10.5772/intechopen.99715.

[79] Grzegorczyk-Frańczak M, Barnat-Hunek D, Andrzejuk W, Zaburko J, Zalewska M, Łagód G. Physical properties and durability of lime-cement mortars prepared with water containing micro-nano bubbles of various gases. Materials 2021;14:1902. https://doi.org/10.3390/ma14081902.

[80] Han S, Zhang P, Zhang H, Kang D, Wang X. Physical and mechanical properties of foamed concrete with recycled concrete aggregates. Front Mater 2023;10. https://doi.org/10.3389/fmats.2023.1106243.